

# Online Research @ Cardiff

This is an Open Access document downloaded from ORCA, Cardiff University's institutional repository: <http://orca.cf.ac.uk/131325/>

This is the author's version of a work that was submitted to / accepted for publication.

Citation for final published version:

Quaglia, Roberto 2020. A review of technologies and design techniques of millimeter-wave power amplifiers. *IEEE Transactions on Microwave Theory and Techniques* 68 (7) , pp. 2957-2983. 10.1109/TMTT.2020.2989792 file

Publishers page: <http://doi.org/10.1109/TMTT.2020.2989792>  
<<http://doi.org/10.1109/TMTT.2020.2989792>>

Please note:

Changes made as a result of publishing processes such as copy-editing, formatting and page numbers may not be reflected in this version. For the definitive version of this publication, please refer to the published source. You are advised to consult the publisher's version if you wish to cite this paper.

This version is being made available in accordance with publisher policies. See <http://orca.cf.ac.uk/policies.html> for usage policies. Copyright and moral rights for publications made available in ORCA are retained by the copyright holders.



# A Review of Technologies and Design Techniques of Millimeter-Wave Power Amplifiers

Vittorio Camarchia, *Senior Member, IEEE*, Roberto Quaglia, *Member, IEEE*, Anna Piacibello, *Member, IEEE*, Duy P. Nguyen, *Member, IEEE*, Hua Wang, *Senior Member, IEEE*, Anh-Vu Pham, *Senior Member, IEEE*

**Abstract**—This paper reviews the state-of-the-art of millimeter-wave power amplifiers, focussing on broadband design techniques. An overview of the main solid-state technologies is provided, including Si, GaAs, GaN and other III-V materials, and both field-effect and bipolar transistors. The most popular broadband design techniques are introduced, before critically comparing through the most relevant design examples found in the scientific literature. Given the wide breadth of applications that are foreseen to exploit the millimeter-wave (mm-wave) spectrum, this contribution will represent a valuable guide for designers who need a single reference before adventuring in the challenging task of mm-wave power amplifier design.

**Index Terms**—Broadband, millimeter wave, power amplifiers.

## I. INTRODUCTION

THE millimeter-wave (mm-wave) spectrum is attracting a great interest for applications such as 5G and future satellite communications that go well beyond the traditional niche of military and scientific use in terms of investments and potential revenues. The most attractive feature of mm-waves compared to the RF and microwave band is the huge spectrum availability that gives a great advantage in terms of capacity for telecommunication systems. Other advantages of mm-wave systems are the compact size of circuits, especially antennas, and the intrinsic easiness of frequency reuse thanks to the high free-space attenuations. There are also some advantages that are band-specific; for example, the very high attenuation in the 60 GHz band due to oxygen absorption that enables intrinsically secure communications.

On the other hand, the very high frequency of operation poses significant challenges to system and circuit design. Similarly to what happens at lower frequency, one of the most critical circuit components is the power amplifier (PA). Its

main figure of merit (FoM) is the output power that must be reached while respecting other requirements such as linearity and power consumption. At mm-wave, the power losses, the sensitivity to components' tolerance, and the physical limitations of transistor technologies make the PA design even more challenging than at lower frequencies.

While these challenges represent an obstacle to an immediate deployment of functional and affordable mm-wave systems, they are very welcomed by the high-frequency PA community who has found an interesting space for the research and development of innovative technologies and techniques that can supplement the knowledge developed for lower frequency PAs.

This paper reviews the evolution and State-of-the-Art (SoA) of mm-wave solid-state PAs, with a particular emphasis on broadband solutions. The term broadband is relative and somehow subjective; this paper focusses on PA examples that generally achieve at least a 10% fractional bandwidth.

The paper is organized as follows. Section II gives a brief overview of the available solid state technologies for power amplification at mm-wave frequency, while Section III summarizes the most common broadband PA design techniques and describes their advantages and limitations. Sections IV to VII critically describe some relevant examples of PAs published in scientific journals or conferences, each section covering a portion of the mm-wave spectrum, according to IEEE radar bands [1]. Finally, Section VIII concludes the paper.

## II. TECHNOLOGIES

One of the most important characteristics of a transmitter is the covered range, which depends on the product of the antenna gain and the PA output power and translates into circuit specifications in terms of PA performance. Although the total transmitter power can be combined from a number of PAs, it is still strictly related to the power density of the transistor technology adopted in the PA. For this reason, power density measured at the mm-wave frequency of interest is a crucial FoM for technology comparison. The other key characteristic of a PA is its ability to amplify, meaning that the gain the transistors can achieve when providing the desired output power is another crucial FoM. The gain is related to transistor characteristics such as the cut-off frequency ( $f_T$ ) and maximum oscillation frequency ( $f_{MAX}$ ). However, power density plays again an important role, since displacement current effects result in an equivalent capacitance that is roughly proportional to the transistor active area. This means

Manuscript received XX XXXX, 2019; accepted XX XXXX, 2019. Date of publication MM DD, YYYY; date of current version MM DD, YYYY.

V. Camarchia is with the Department of Electronics and Telecommunications, Politecnico di Torino, C.so Duca degli Abruzzi, 10129 Torino, Italy. e-mail: vittorio.camarchia@polito.it

R. Quaglia is with the Centre for High Frequency Engineering, Cardiff University, Queen's Buildings, The Parade, Cardiff CF24 3AA Wales, UK. e-mail: quagliar@cardiff.ac.uk

A. Piacibello is with the Department of Electronics of the University of Roma Tor Vergata, via del Politecnico 1, 00133 Roma Italy and the Department of Electronics and Telecommunications, Politecnico di Torino, C.so Duca degli Abruzzi, 10129 Torino, Italy. e-mail: anna.piacibello@polito.it

Duy P. Nguyen is with MACOM Technology Solutions, Santa Clara, CA, USA e-mail: duy.nguyen@macom.com

H. Wang is with the Georgia Institute of Technology, Atlanta, GA, 30308 USA e-mail: hua.wang@ece.gatech.edu

A. V. Pham is with the Department of Electrical and Computer Engineering, University of California at Davis, Davis, CA, 95616 USA e-mail: pham@ece.ucdavis.edu

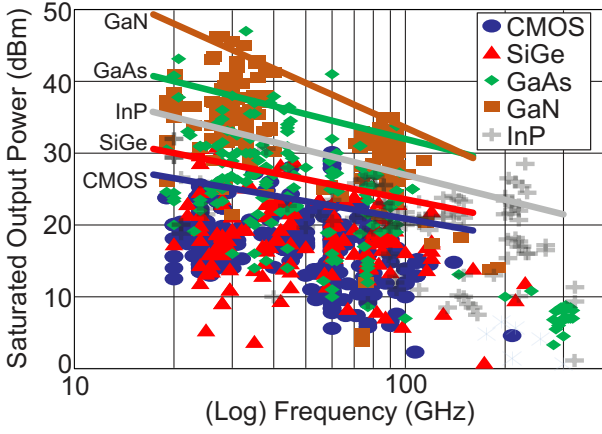


Fig. 1. Survey of published PAs from K-band to over 300 GHz, extracted from [2]. Saturated output power versus frequency of operation for different transistor technologies.

that for the same output power target the transistor with better power density will have lower capacitance hence, assuming the real part of the load is the same in both cases, it will be easier to use in high frequency, broadband PAs with good gain.

Power efficiency and linearity are notably linked; their trade-off, that arises when linearity is a strict system constraint, is difficult to optimize at transistor level, so circuit level solutions must be sought. However, if considered independently, linearity is deeply linked to the transistor characteristics such as the transconductance profile, the presence of traps, and the dynamic non-linearities. At the same time, the efficiency is also deeply affected by some transistor characteristics such as the ratio between drain bias and knee voltage. Moreover, the adoption of circuit solutions to improve efficiency, such as harmonic tuning, relies on the ability of the transistor to *i*) generate drain current profiles with sufficient harmonic content, i.e., that are sharp enough, meaning high speed transistors, and *ii*) sustain the resulting voltage waveforms, i.e. with sufficiently high breakdown voltage.

By keeping in mind the above considerations, the survey result shown in Fig. 1 is not surprising. It reports the output power versus frequency performance of an extended database of published PAs, extracted from the survey maintained at Georgia Tech [2]. In particular, Fig. 1 focusses on PAs in Ka-band and above, while the original survey includes microwave and RF bands, as well as multipliers and oscillators. The different markers and colors refer to different technologies, with corresponding trend lines. To be noted; the trend lines are not regression lines, but a tentative to capture the best efforts for each technology, not considering however the single cases which exceed considerably the general trend.

What makes a successful technology or product is delivering value to the end-user, and no single semiconductor technology achieves the optimal balance in every application. III-V compound semiconductor technologies (sketch of typical device cross-sections in Fig. 2), particularly GaAs and GaN, offer exceptional power density, gain and efficiency over a broad frequency range, providing system/design engineers with a wide

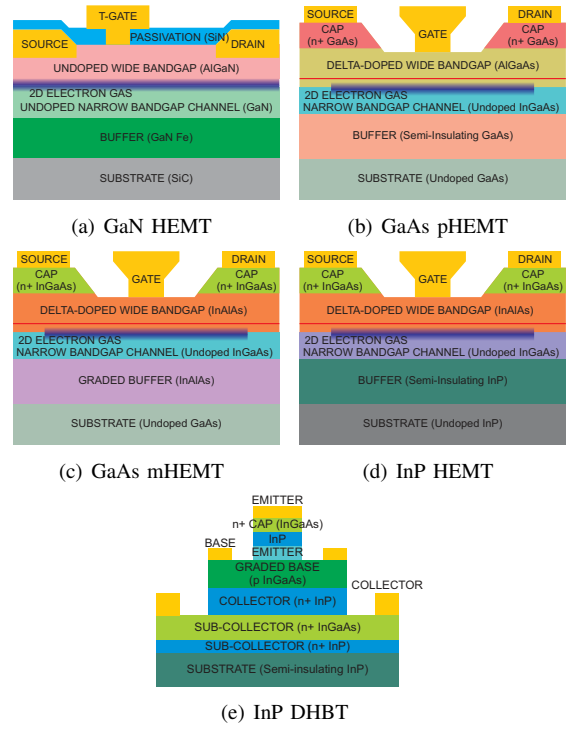


Fig. 2. Sketch of mm-wave high electron mobility transistor structures in III-V material systems.

trade-space to achieve optimal PA performance and economic value. In addition to their inherent performance advantages, and driven by smartphone demand, these technologies have achieved the economies of scale to satisfy the expected volume requirements of emerging mm-wave applications [3], [4]. On the other hand, silicon technologies (typical device cross-sections in Fig. 3) can rely on great advantages in terms of integration and they are the technology of choice for medium and lower power levels.

### A. III-V technologies

GaN devices for mm-wave are High Electron Mobility Transistors (HEMTs) with aggressive gate scaling, ranging from 150/100 nm in commercially available processes down to 20 nm at research level [27], corresponding to  $f_T$  between 50-70 GHz and up to 300-400 GHz, respectively. This scaling is achieved by adopting T-gate processes, and supported by ad-hoc design of the epitaxial layers and Schottky contacts. Comparable performance with InP and GaAs in terms of gain and noise figure can be observed while maintaining high breakdown voltage, of particular interest in transceiver integration [32], [33]. Fig. 1 shows that the trends of GaN and GaAs converge at around 150 GHz, with the GaN trend line dropping faster than GaAs. The main reason for this is likely to be the higher maturity of GaAs technology that allows for a better current density. In our opinion, GaN technology still has margins for growth and will become the technology of choice when raw power at mm-wave is the main target, while HBTs scaling may make these technologies more attractive than HEMTs beyond 100 GHz. Substrate selection is a critical

TABLE I  
PROCESS PARAMETERS OF SEVERAL TRANSISTOR TECHNOLOGIES

Technology	Gate length/Emitter width (nm)	$f_T$ (GHz)	$f_{MAX}$ (GHz)	GD/CE Breakdown (V)	Power density (mW/mm)	Ref.
GaAs pHEMT	250	45–70	90–100	18–20	700–1200	[5]
	150	70–85	120	12–16	560–1000	[6]
	100	130	185–200	5–9	250–850	[5]
GaAs mHEMT	125	150	250	8	30	[7]
	100–30	200–515	380–1000	4–2	-	[7]–[10]
InP HBT/DHBT	512–500	250–370	390–490	4–4.9	-	[8], [9], [11], [12]
	256–250	375–520	650–850	4	500	[6], [11], [13]
	128	730	1300	3.3	-	[11]
InP HEMT	100	120	500	5.5	-	[14]
	80	300	700	-	-	[10], [13]
SiGe HBT/BiCMOS	180	170–180	200–250	1.6	-	[15]
	130–120	200–270	260–450	1.6–3.5	-	[16]–[21]
GaN/Si HEMT	100	100	180	25–50	3300–4000	[7], [22]
	60	150	190	25–30	3000	[7]
GaN/SiC HEMT (power)	200	40	100	-	3400	[23]
	150	35–80	120	70	3500–4000	[5], [24], [25]
	100	140	-	-	2000	[26]
GaN/SiC HEMT (high freq.)	150 (T2)	90	220	50	-	[27]
	40 (T3)	200	400	40	300	[27]
	20 (T4)	330	550	17	-	[27]
Si CMOS/SOI	120	196	230	-	-	[28]
	90	243	208	2.5–3	-	[29]
	45	300–400	350–500	-	50	[28], [30], [31]

issue in GaN. High performance GaN devices are grown on SiC substrate that is known for its high cost. As a consequence, several groups have focussed on GaN on Si substrate as viable solution for mass-market applications, and commercial products are already available. On the other hand, Si substrates have worse electrical and thermal performance compared to SiC substrates, and the compromise performance versus cost must be evaluated at system/product level. Also, the choice between high- or low-resistivity substrates is source of debate and research [34]. Low-voltage GaN, although still at research level, is interesting for mobile user applications since it would bring some of the advantages of III-V technology but at a reduced cost compared to GaAs, mainly thanks to the possibility of integrating on a Si substrate.

GaAs-based processes can still be considered the prime choice in mm-wave applications when a significant amount of power is needed. Fig. 1 shows how spread in both power and frequency the presence of GaAs PAs in literature is, a clear indicator of the great flexibility offered by GaAs that enables its use in different scenarios. The two main epitaxial structures used are pseudomorphic HEMTs (pHEMT) and metamorphic HEMTs (mHEMT). The gate lengths vary from 150 nm for K-bands applications, to 100 nm to cover applications up to 100 GHz for pHEMTs, while mHEMT-based PAs with the same gate length are found up to 160 GHz [35]. mHEMTs with gate length of 35 nm allow PA design up to 300 GHz [36].

InP- based technology is the only one currently able to provide PAs with >20 dBm output power above 200 GHz [37]–[41]. Bipolar transistors (Heterojunction Bipolar Transistors (HBT), and Double-Heterojunction (DHBTs)) have been used to design PAs up to 325 GHz, while HEMT-based PAs have been presented up to 185 GHz, with gate length of 80 nm [13].

The DHBT 500 nm and 250 nm technology nodes provide  $f_T$  around 330 GHz and 400 GHz, respectively, the latter with an  $f_{MAX}$  up to 700 GHz. HEMTs with gate length of 50 nm give  $f_T$  around 600 GHz, however with similar  $f_{MAX}$ . The main limitation of InP is its cost, due to the difficulty in sourcing In and because it is a very brittle material, making its manufacturing and handling extremely perilous.

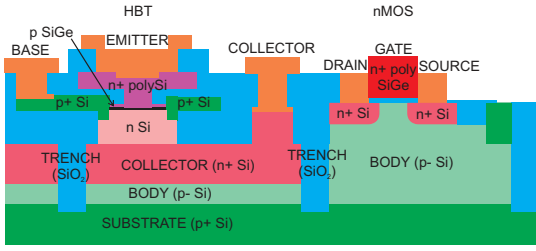
### B. Si and SiGe technologies

Si-based PAs clearly struggle to achieve the same power versus frequency performance of the III-V competition, but they are unbeatable in terms of cost (when mass-produced) and integrability. Also, they are competitive in terms of frequency alone, with examples up to 230 GHz in SiGe HBT [42] and up to 210 GHz in Si on Insulator (SOI) Complementary Metal-Oxide-Semiconductor (CMOS) [43].

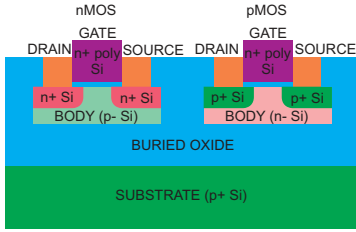
CMOS technology for mm-wave PAs relies on extreme gate scaling, from 180 nm down to 28 nm and beyond. However, the frequency of operation is not always the main drive for choosing the gate length, but sometimes other considerations such as cost and the ability to integrate with the rest of the transceiver are guiding the selection. A clear example are 40 nm CMOS PAs and 45 nm CMOS SOI PAs that are being developed for 5G at around 28 GHz [30], [44], where longer gate CMOS PAs are still capable of operating, although with lower performance [45]. The main conundrum to be solved is related to the most evident drawback of scaling down the technology that is the breakdown voltage reduction. Although circuit design techniques might help mitigating this problem, such as transistor stacking, they never come for free and lead to increased parasitics that affect maximum frequency as well as achievable energy efficiency and linearity.

BiCMOS technology is intrinsically an example of integration, since it combines bipolar and field-effect transistors on





(a) SiGe BiCMOS



(b) SOI CMOS

Fig. 3. Sketch of mm-wave transistor structures in Si and SiGe.

the same substrate. The technology nodes typically used at mm-wave range from 250 nm with  $f_T$  around 220 GHz [46], down to 90 nm with  $f_T$  of 300 GHz [47]. BiCMOS can be used for analogue Intermediate Frequency (IF) and baseband functions as well, and the CMOS part supports Digital Signal Processing (DSP) functions.

Integration is, in the view of the authors, the main advantage of Si technology. With up to ten metal levels, the capability of producing very complex circuits is unrivalled. Also, the performance of passive elements in terms of losses or quality factor is quite competitive [47]. The cost advantage however becomes clear only for mass produced parts, since the initial costs are much higher than in III-V technologies.

### C. The 5G array scenarios

The high capacity services of 5G will use the mm-wave spectrum with the so called 5G New Radio (5G-NR) [48]. Fig. 4 reports the bands assigned by 3GPP (TS 38.101-2) to the Frequency Range 2 (FR2) of the 5G-NR. Two distinct set of bands can be observed. The first one, around 27 GHz, includes the n257, n258 and n261 bands; therefore, a transmitter aiming to cover this set will need to be designed over 24–30 GHz, corresponding to a 22% fractional bandwidth. The n260 band, around 38.5 GHz, extends from 37 to 40 GHz, requiring a 8% fractional bandwidth. The biggest change compared to existing systems at mm-wave is however the unprecedented requirement for very large instantaneous bandwidths. In fact, the channel widths supported are, for FR2, up to 400 MHz per carrier, with the option of having multiple carriers and with practical requirements for the base-station side up to 1 GHz being considered at the moment. This puts quite a lot of stress on the PA design from an equalisation point of view, since it cannot be expected from predistorters to correct excessive amounts of in-band gain variations. However, even more important is to guarantee uniform non-linear characteristics (AM-AM and AM-PM) on such a large bandwidth. At the same

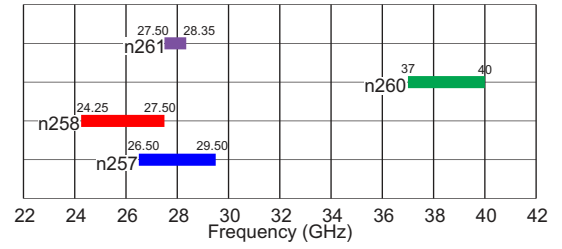


Fig. 4. Frequency Range 2 designation for 5G NR.

time, the baseband impedance must be controlled accurately up to a frequency of 3-5 times the channel bandwidth to eliminate memory effects. This means that bias networks must be resonant free potentially up to 5 GHz, stressing the requirements for on- and off-chip by-pass circuitry.

From a transmitter architecture point of view, base-stations will be based on active antenna arrays with a considerable number of elements to allow for beam-steering and/or beam-forming. The type of array architecture will be a deciding factor in the selection of the PA technology. In fact, if many antenna elements will be clustered and fed by a single PA, or in case of analog beam-forming, higher power technologies will be preferred, and GaN could be regarded as the winning solution. On completely the other hand, if each single radiator will be fed by a separate transceiver, as in digital beam-forming arrays, then Si-based technology makes more sense. In the short term, however, the system cost for the latter case is still too high due to its enormous complexity in both front-end and back-end, making this solution unpractical. Therefore, while current real-field 5G systems employ CMOS based active array configurations [49], hybrid beam-forming arrays [50] are likely to become the short term solution for 5G NR, and GaAs might actually be the winning solution for the PA (and perhaps the TX/RX switch and LNA), with the rest of the transceiver made on BiCMOS technologies.

### III. DESIGN TECHNIQUES

High frequency PAs at these frequencies are mostly based on reduced current conduction angle modes, typically class AB to maintain a good compromise between linearity and efficiency. Class C is used on its own when linearity is not a concern, for example in radar and imaging, or in complex architectures such as the Doherty PA [51], [52].

Reactive matching is the standard solution for presenting the optimum load at the transistors. Due to the displacement current, each transistor will present an output capacitance; this leads to the inability to perfectly match it over an arbitrary bandwidth, known as the Fano limit [53]. At mm-wave, wideband reactive matching is suitable for medium bandwidth with the benefit of easy design and well predictable performance. The practical limit is the number of matching sections that can be used due to the impact of their losses, leading to a compromise between matching accuracy and insertion loss. To partially alleviate this, the matching network design can be based on the continuous PA modes theory [54]. Although developed as a general concept and demonstrated

at RF and microwave frequencies [55], [56], it has already found application at mm-wave frequencies, as for example in [57], [58]. While for an application of textbook continuous mode theory the harmonics must be controlled precisely, the practical advantage that they bring is the understanding that matching requirements can be relaxed by accepting a slight and controlled reduction of performance [59]. One drawback of continuous modes, and of most of harmonic manipulation techniques, is that they require the active devices to sustain voltage waveforms with high peaks. While this might be acceptable in technologies like GaN where the breakdown is much larger than twice the bias voltage, it might represent a limitation for low voltage technologies where bias voltage reduction will lead to lower output power density.

Independently of the technology adopted, single transistors are mostly unable to provide the required level of output power, therefore some form of power combining is necessary. Multi-finger transistors are the obvious first step. GaN technology has the potential to provide Watt-level output power with a single multi-finger transistor cell. There is a limit, however on the number of fingers that can be fed by a single gate access, due to the need of keeping parasitics under control, especially due to phasing and long source connections. Corporate combiners are the most common in III-V technology [35], [41], [60] but used also in Silicon [61], and they are a form of parallel (or current) combining. Based on fork combiners, normally in a binary arrangement, they provide both power combining and matching functions. A common way of designing these even-mode combiners is to start from a multi-stage ladder matching network that matches an equivalent device ( $N \times 1$ ) which represents the total periphery, as if the  $N$  individual devices to be combined were in parallel, and then split the components in symmetric arrangements to achieve the desired combiner (see Fig. 5(a)–(c)). To combine  $N$  identical devices having optimum load resistance  $R_{OPT}$  and equivalent output capacitance  $C_{OUT}$ , the equivalent  $N \times 1$  device with the total periphery will have optimum load resistance  $R_{OPT}/N$  and equivalent output capacitance  $N \times C_{OUT}$ . This approach does not affect bandwidth, at least in principle, but it requires optimisation when real component will be placed in. A semi-lumped implementation is often preferred in MMICs, where the series inductors are replaced by equivalent distributed elements (TLs in Fig. 5(d)). This, however, has an impact on bandwidth, and requires a re-tuning of the values since the transmission lines will also absorb some capacitance. The main drawback of this solution is the extensive use of shunt capacitors whose accuracy and repeatability becomes a key requirement for the MMIC process. Off-chip power combining is also possible, and gives great flexibility. Bulk waveguide combiners are the most common choice, but sometimes off-chip combination on a substrate is also used (mainly to save area on precious MMIC substrates). An example using both waveguide and microstrip combiners can be seen in [62] for a V-band PA module. This solution is very interesting at higher mm-wave bands, where the dimensions of the air combiners is very small.

An interesting alternative for broadband design is the use of balanced PAs. While at microwave frequencies the use of

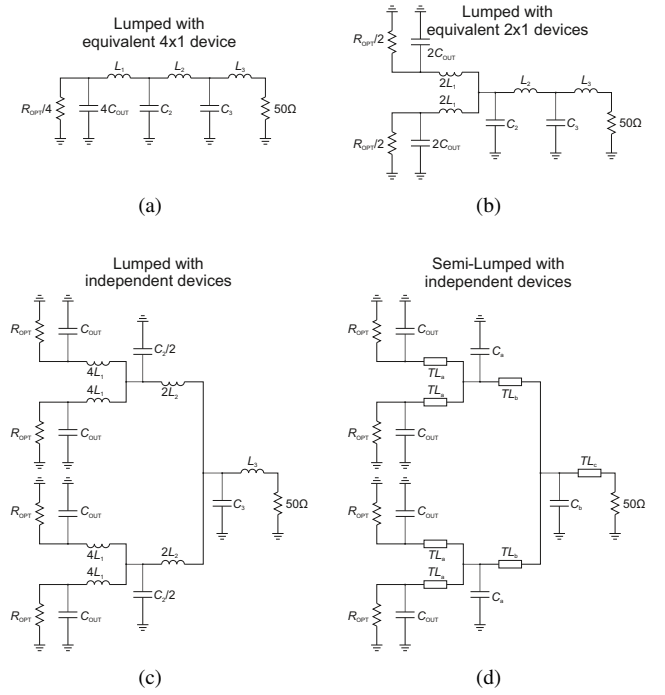


Fig. 5. Simplified diagrams showing the design procedure of even-mode corporate combiners for the case  $N = 4$ , where the individual device has optimum load resistance  $R_{OPT}$  and equivalent output capacitance  $C_{OUT}$ .

Lange couplers is sometimes seen as a problem due to their size and aspect ratio, at mm-wave they are very small and they provide a much better design environment than corporate combiners. There is a technology challenge, however; wafers for mm-wave applications above Ka-band are usually thinned to  $50 \mu\text{m}$ , meaning that width and spacing of Lange fingers must be brought down to a challenging  $4 \mu\text{m}$  to achieve the right ratio between odd- and even-mode impedance in broadband design. Alternatives exist, and broadside coupling can be adopted instead of edge coupling to obtain 3 dB couplers; in III-V technology this might require to use soft dielectric layers to build the spacer between the coupled lines [36]. Normally, a combination between even mode combining and balanced structures is adopted, as depicted in Fig. 6. An advantage of this configuration if compared with the corporate combiner of Fig. 6 is the reduced impedance transformation ratio required, with possible improvement of bandwidth. This is true if the Fano limit is not being approached. The Fano limit depends solely on the  $Q$ -factor of the load to be matched that is almost independent on periphery, since the resistive part decreases, but the capacitive part increases, with increasing device size. The other advantages are related to the use of balanced structures in general, such as the inherent isolation between stages and the possibility of achieving simultaneous flat gain and good matching over a wide bandwidth. On the other hand, couplers generally introduce more loss than corporate combiners, and normally complicate the routing of the bias voltage since they naturally block DC between the stages. Push-pull is a differential power combining technique that ideally combines two class-B PAs to reconstruct a full-wave

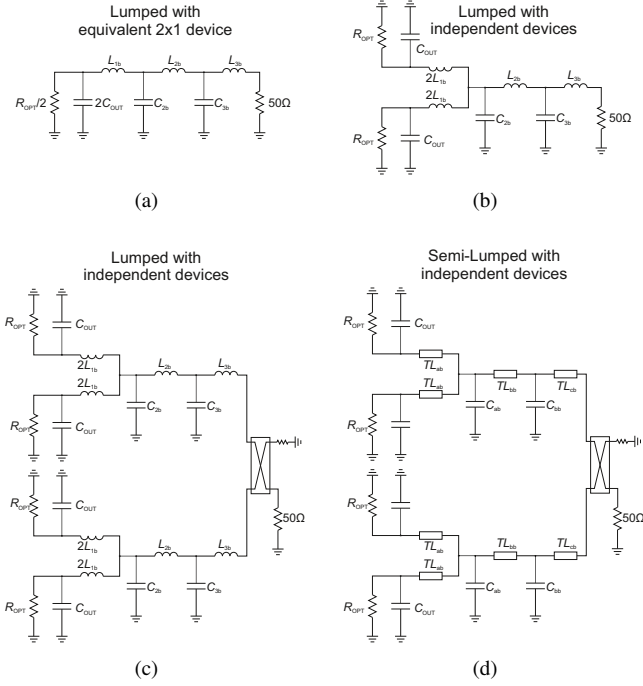


Fig. 6. Simplified diagrams showing the combination between corporate and balanced combining.

at the output, therefore eliminating the need of even harmonic resonators and improving the bandwidth. Since most systems require a single-ended output, the output signal is obtained through a balun transformer. This normally brings other advantages since it theoretically provides a  $25\ \Omega$  impedance at the amplifier ports, favouring the impedance ratio for matching. In reality, due to the limited coupling coefficient and self-loading, a  $25\ \Omega$  impedance can be achieved but is not readily present. Numerous push-pull PA examples are found at mm-wave frequencies, in particular in GaAs [63], [64] and CMOS [65], [66]. On the other hand, power combining through transformers is a common feature in CMOS and BiCMOS design [67]–[69] thanks to the exploitation of the many metal layers available to realize 3D broadside transformers whose parasitics effects are reduced compared to planar transformers. Series combination through transformers is used also in III-V PAs [70].

The main limitation with parallel combining in low-voltage technologies is that optimum impedance decreases almost linearly with the increasing number of transistors, affecting the achievable bandwidth due to a larger impedance ratio to match. An intuitive strategy to reduce the impedance ratio is transistor stacking that ideally corresponds to voltage combining. In particular, the transistors are stacked, starting from a bottom stage with grounded source/emitter, and connecting on top a number of transistors. Parallel and stacking configurations are compared to a single stage configuration in the simplified schematics of Fig. 7. It can be noted how the idealised matching network connected at the output scales differently in the two cases, with the advantage of lowered impedance ratio and capacitance compared to the parallel combining case. This

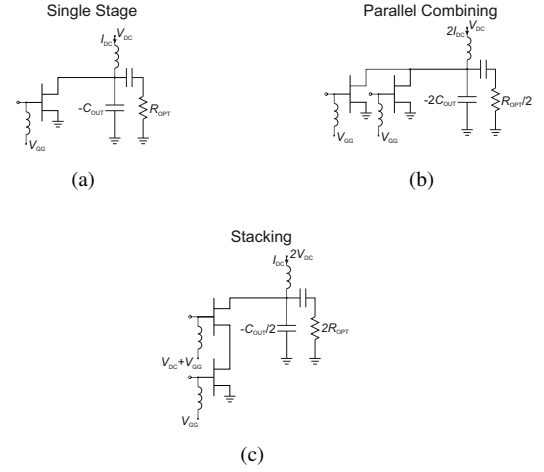


Fig. 7. Simplified diagrams for (a) single-stage, (b) parallel combining and (c) stacking showing the effect on an idealised output matching.

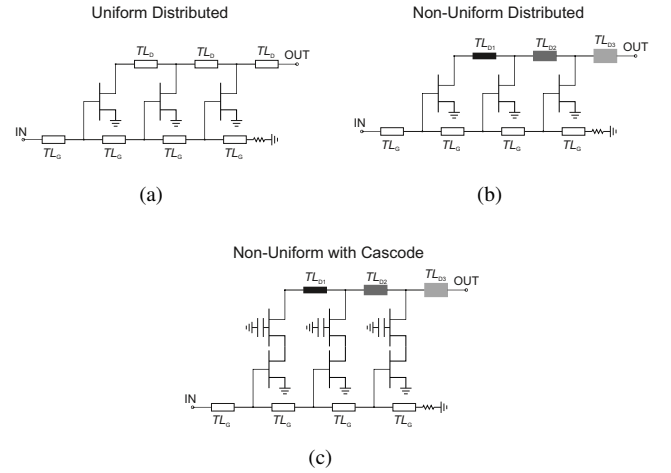


Fig. 8. Simplified diagrams for different distributed amplifier solutions.

technique is almost a standard in CMOS [71] and BiCMOS PAs (with better stacking possible in SOI technologies), but it is used for GaAs as well [72], [73]. GaN stacking might be employed effectively for short gate transistors. For example, for 100 nm HEMTs, that work at around 15 V bias, stacking might become useful to reach an output power higher than 10 W.

Distributed amplifiers allow to achieve very broadband design by exploiting a very simple but powerful concept. When considering a capacitively-loaded transmission line, the bandwidth on which the structure behaves like a normal transmission line can be enhanced by increasing the number of loaded sections per unit length. The distributed amplifier uses this concept by loading two transmission lines, at input and output, with the transistors' gate and drain capacitances, respectively. By equalizing the delay at input and output between each transistor, the distributed amplifier can achieve amplification on a very broad frequency band. As a consequence, they are the topology of choice for applications such as radar countermeasures and optoelectronic modulator drivers. Schematic

diagrams of three different distributed amplifier configurations are shown in Fig. 8. The uniform distributed amplifier provides good bandwidth but generally does not show good efficiency and does not maximise the output power. The reason is that the devices are not seeing a uniform voltage swing along the structure, since the voltage builds-up along the output line-up, with the one further away from the load having the lower voltage swing and therefore lower output power and efficiency. The non-uniform distributed power amplifier (NDPA), on the other hand, uses pieces of transmission line with different impedance (decreasing towards the load) to achieve a more uniform voltage swing along the structure and therefore a better output power and efficiency for all devices. Also, it is very common to substitute the transistors with Cascode cells in order to decrease the input capacitance of each amplifying unit, thus increasing gain and bandwidth of the distributed amplifier. Examples of distributed amplifiers can be found both in III-V [9], [74]–[78] and Silicon-based PAs [79]–[82].

The NDPA [83], [84] was initially proposed in the 1980s adopting GaAs devices. However, the low output power (typically lower than 30 dBm) limited its application and favoured reactively matched topologies. The advent of GaN MMICs increased the achievable output power on one side, but limited the bandwidth achievable by reactive matching due to the high-Q terminations required. This paved the way for the rediscovery of the NDPA topology for wideband GaN PAs.

There are also variants to the traditional distributed amplifier, for example the constructive wave amplifier, where drain and gate are loading the same transmission line [85].

#### IV. K-BANDS (18–40 GHz)

The low portion of the mm-wave spectrum (more properly cm-wave/mm-wave) is covered by the K-bands (K-band 18–26.5 GHz and Ka-band 26.5–40 GHz). In the past, these bands were exploited mainly for radar and backhaul applications, while more recently they have become attractive also for other strategic applications relevant to a large number of emerging mass-markets like satellite communications and, most importantly, 5G mobile communication.

Regarding 5G, the bands around 28 and 39 GHz have been identified (see e.g. the 3rd Generation Partnership Project (3GPP), released December 15, 2017 [86] and following) as the best candidates for the initial fixed deployment (commercial deployments expected to start in 2020).

Normally, conservative design approaches are used at these frequencies, resulting in mm-wave PAs with poor efficiency. The reason is that low-frequency well-established design and characterisation techniques, such as harmonic load-pull and waveform engineering, are still being explored at mm-wave. In terms of signal bandwidth, the present trend is toward bandwidths from 800 MHz to more than 1 GHz. This opens up the potential to utilize the same portion of the spectrum, and therefore the same equipment, not only for mobile broadband access, but also for backhaul, to simplify small cells deployment. On the other hand, the power consumption of individual wireless devices and back/base stations in 5G networks must be minimised to cope with the billions of connected devices

TABLE II  
PA SATURATED OUTPUT POWER REQUIREMENTS FOR COMMERCIAL APPLICATIONS IN K- AND KA-BANDS.

Application	Freq. (GHz)	Power (dBm)	Technology/ies	Ref.
Backhaul	18–26	23–36	GaAs	[88]
	26–38	20–33	GaAs, GaN	
5G NR	24.25–27.50	10–20	CMOS, SiGe,	[86]
	26.50–29.5			
	27.50–28.35 37.00–40.00	30–40	GaAs, GaN	
Radar	24.05–24.25	10–20	CMOS, SiGe	[1]
	33.4–36			
Satellite	17.3–22.0	37–50	GaAs, GaN	[89]
	27.5–31			

and enable a reduction in energy usage over existing 4G networks [87].

The applications identified differ mainly in terms of power requirements, driving the choice of the adopted technology and the complexity of the PA architecture. They span from around 10–20 dBm for radars up to 37–50 dBm required by satellite applications. For 5G and backhaul, the power levels are still partially under definition, but two sub-ranges can be identified, depending on the transmitter architecture in terms of the analog or digital beam-forming scenarios. Table II reports, for the identified applications, the technologies that can achieve the required power at MMIC level, without the need of off-chip combiners.

##### A. Standard PAs

In 1986, Kim *et al.* presented the first millimeter-wave MMIC PAs at 44 GHz: a single stage amplifier with 10 dB gain and a parallel-combined topology with over 17 dBm saturated power and a power density of 23 dBm/mm adopting 300 nm GaAs FETs [90].

The first examples of K-bands MMIC PAs appeared around the early 90s do not target a specific application, but are suitable for radar, communications, smart munitions or local multipoint distribution services (LMDS). The technology node of choice in the first decade was 150 nm GaAs, which enabled to achieve from 18 dBm up to roughly 38 dBm above 30 GHz. The architectures of these examples are based on combined or balanced devices, mostly adopting two stages to increase gain. In [91], a complete on-chip transceiver working up to 40 GHz developed by TRW Inc. is reported. The PA achieves 18 dBm output power with 12 dB gain from 37 to 40 GHz. Fig. 9 reports, still by TRW Inc., a power module combining two GaAs MMIC power amplifiers (two stages) and a driver (two stages) to achieve the record output power of 37.7 dBm at 34.5 GHz, with a corresponding efficiency of 24% and a small-signal gain of 22 dB [92]. The technology was not mature enough to realize a single chip, mainly due to the losses of the combining and matching networks, which were realised off-chip as highlighted in Fig. 9.

Full on-chip power combining in GaAs is achieved in [93], [94]. Both PAs, developed by TRW Inc., adopt the same two-stage architecture reported in Fig. 10, where both driver and power stages are balanced amplifiers. To achieve the required



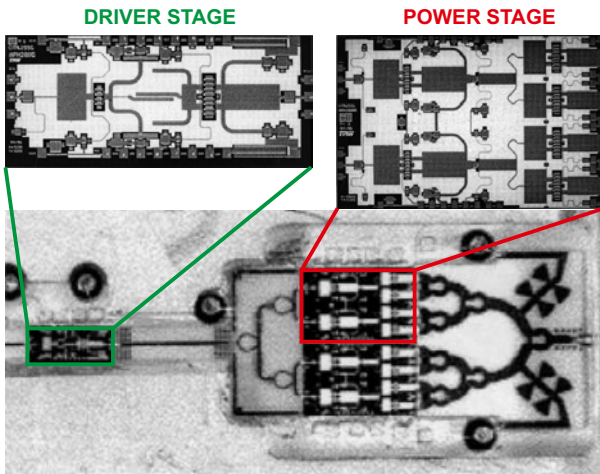


Fig. 9. 34.5 GHz 150 nm GaAs power module combining two MMIC PAs and a driver [92] ©IEEE 1997.

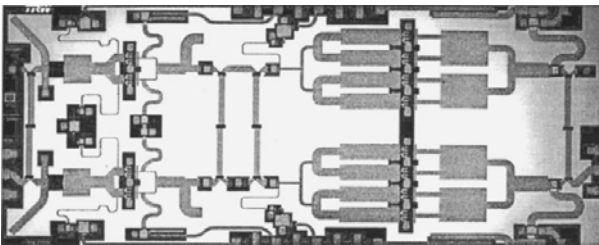


Fig. 10. 150 nm GaAs single-chip MMIC power amplifier [93] ©IEEE 1998.

power level, devices are parallel-combined both in the driver and the power stages. In [93] the target application is LMDS, covering the 27.5–29.5 GHz band, where the PA maintains a saturated output power and PAE higher than 32 dBm and 32%, respectively. The MMIC in [94] is one of the first examples targeting ground terminal satellite applications. It achieves a saturated output power and PAE higher than 32 dBm and 22% over a 3 GHz bandwidth, from 29 to 32 GHz, demonstrating the feasibility to fully cover the uplink satellite band with this technology. This PA shows a substantial bandwidth increment compared to [93] without compromising the performance.

Broadband PAs achieving more than 10 GHz bandwidth can be found since 2000. Even if different design strategies are applied, e.g. distributed in [95], three-stage PA adopting single devices in [96] and two-stage balanced in [97], a common feature of these examples in 250 nm GaAs is the limited output power (below 23 dBm), possibly requiring off-chip combining to achieve Watt-level operation. A novel strategy to achieve broadband operation is proposed in [98], where the parasitic drain capacitance of the active devices is absorbed into the output matching/combining network, which also provides some immunity to process variations. The single-stage PA adopting two 150 nm GaAs pHEMTs parallel-combined with coupled resonators demonstrates 22.5 dBm output power, 30% PAE and 10 dB gain from 17 to 35 GHz.

A lower power (17 dBm), though on a wider bandwidth (26–40 GHz), is achieved in [17] on 130 nm SiGe BiCMOS.

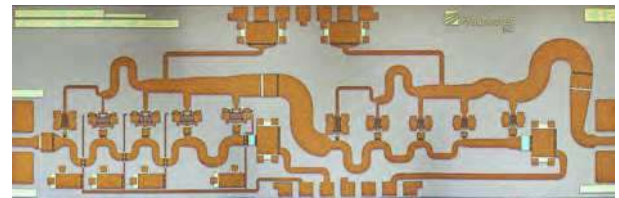


Fig. 11. 100 nm GaN/Si MMIC two-stage distributed power amplifier [99] ©IEEE 2014.

This two-stage differential PA features 10 dB gain and is compatible with satellite and ground-based communications and radar applications. However, its PAE is limited to 5% over the whole bandwidth due to the adoption of a linear class of operation (class-A). Conversely, the highest power in SiGe is demonstrated in [15], a combined PA which can ensure around 30 dBm output power with PAE higher than 13% from 20 to 28 GHz. Even wider bandwidth (12–40 GHz) is achieved by adopting the distributed topology in 130 nm SiGe BiCMOS [18], which achieves 19 dBm output power while maintaining PAE higher than 8%.

The advantages of the rising GaN technology in terms of power density directly reflect on the performance of [99] (Fig. 11). This two-stage distributed PA in 100 nm GaN/Si covers the 6–37 GHz band with 10 dB gain and output power as high as 30 dBm. Even if the technology was still novel at the time, it achieved a PAE (7%) comparable with the more consolidated SiGe examples. GaN MMIC PAs in K-bands were first demonstrated in 2004 [25], where a 150 nm GaN/SiC ( $f_T > 80$  GHz,  $f_{MAX} > 120$  GHz) process was adopted to realize two similar single-stage prototypes, one in coplanar waveguides (CPW) and one in microstrip, with 4 parallel-combined devices achieving around 32 dBm output power with more than 15% PAE and 8 dB gain at 33 GHz. The evolution of the GaN technology allowed, some years later, to realise more complex structures, both in terms of number of stages and architecture. In 2012, TriQuint presented a 3-stage single-ended PA and its corresponding balanced structure [100] (Fig. 12). The balanced PA maintains output power in excess of 39 dBm, PAE higher than 23% and small-signal gain higher than 20 dB in the range 25–30 GHz, almost doubling the power of the single-ended PA with a limited impact on PAE over the same bandwidth.

In 2015, Northrop Grumman achieved a significant improvement in performance adopting a two-stage structure combining 16 devices in 200 nm GaN/SiC HEMT technology, as shown in Fig. 13. The PA achieves 45 dBm between 26 and 30 GHz, with a PAE higher than 30% and a small-signal gain around 20 dB [23]. The highest power achieved in GaN is in excess of 46 dBm [101], with similar gain and slightly lower PAE over the same bandwidth. In less than 10 years GaN filled the technological gap with respect to GaAs. In fact, the highest power achieved in K-bands by GaAs MMIC PAs is of the order of 38 dBm at 40 GHz [102]. To reach power levels compatible with applications currently covered by travelling wave tubes, of the order of 45 dBm, which is feasible at MMIC level with GaN, GaAs technology requires off-chip combination of

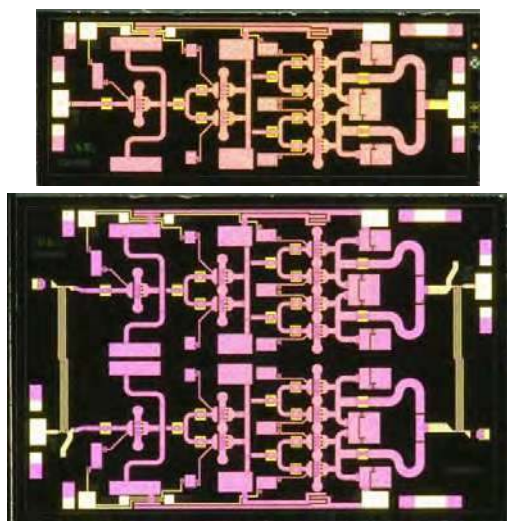


Fig. 12. Single-ended (top) and balanced (bottom) 150 nm GaN/SiC MMIC three-stage power amplifiers [100] ©IEEE 2012.

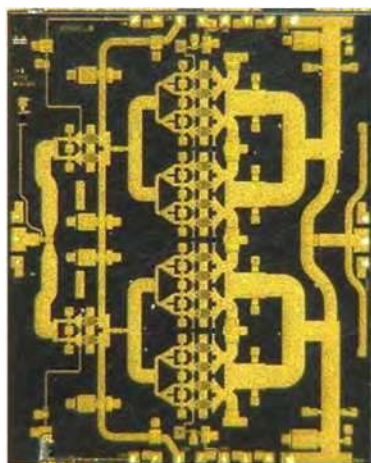


Fig. 13. 45 dBm 16-combined PA adopting 200 nm GaN/SiC HEMTs [23] ©IEEE 2015.

several MMICs, as in [103].

For several years, since its introduction, GaN HEMTs have been fabricated on SiC substrates. Despite their significant cost and limited availability, SiC substrates have enabled complete modules with superior performance with respect to any competitors (mainly GaAs), especially for applications where absolute performance is more important than cost, such as military, satellite and backhaul. A recent example of a broadband, general purpose PA is presented in [26] (see Fig. 14). The PA shows output power in excess of 37.8 dBm, PAE of the order of 25% and small-signal gain of 22 dB between 26 and 35 GHz, thus covering most of the Ka-band. Lately, especially in the framework of analog beam-forming for 5G networks, Si substrates have been explored due to the lower cost and easier integrability of the PA with the digital part of the transceiver, despite having worse thermal properties. In 2018, OMMIC presented a 3-stage combined PA targeting 33 dBm output power and 20 dB gain at 40 GHz

adopting its 100 nm GaN/Si process [22], shown in Fig. 15.

For applications requiring power levels limited to around 20 dBm, K-bands PAs in Si technology appeared around 2005. Before the advent of 5G, the absence of a high-volume application limited it to few examples demonstrated mainly at research level, with PAE mostly limited to below 20% at saturation. Around 2015, the great interest for 5G active antenna arrays exploiting digital beam-forming has boosted the number of solutions proposed based on Si technology, which is favourable in terms of integration and unit cost for mass-applications, and compatible in terms of performance. Stacked transistor cells have been often adopted instead of single common-source and cascode topologies for the PA basic cell.

In [107], the comparison of a common source and a two-stacked PAs designed in 28 nm bulk CMOS at 28 GHz is presented. The two-stacked PA allows for higher gain (13.6 dB) and saturated power (19.8 dBm) in the same chip area ( $0.28 \text{ mm}^2$ ) as the common source stage. High linearity is achieved using a deep class-AB bias point and appropriate harmonic control circuit, demonstrating 25% PAE and -33 dBc adjacent channel leakage ratio (ACLRE-UTRA) at 14.6 dBm average output power with an LTE signal with 16-quadrature amplitude modulation (QAM), 7.5 dB PAPR and 20 MHz bandwidth.

The best performance in terms of saturated power (of the order of 25–26 dBm) and bandwidth is achieved by combined structures [108], [110]. In [108], 4 cascode cells in 90 nm CMOS are combined with transformers as 2 differential amplifier cells, resulting in an extremely compact structure, with a saturated PAE of 27% and gain of 15 dB from 22 to 30 GHz. In [110], a stacked topology in 45 nm SOI CMOS is adopted in a two-stage configuration for each basic cell of the 8-combined PA. The resulting efficiency in the range 33–45 GHz is of the order of 10%.

The inherent low efficiency of Si-based PAs has an even higher impact when non-constant envelope modulation schemes are adopted, like in 5G systems, where the PA is operated most of the time around 6–9 dB of back-off. The

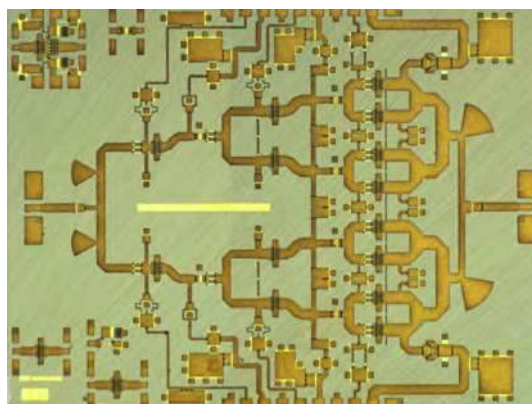


Fig. 14. Broadband 3-stage combined PA in 100 nm GaN/SiC [26] ©IEEE 2019.



TABLE III  
SOA K-BANDS STANDARD PAs.

Ref.	Year	Technology	Freq. (GHz)	Topology	N. of stages	$P_{SAT}$ (dBm)	PAE <sub>SAT</sub> (%)	SS Gain (dB)
[104]	2003	100 nm GaAs mHEMT	32	combined	2	35	40	24
[105]	2004	150 nm GaAs mHEMT	18–40	single-ended	2	9.5	-	20
[102]	2010	300 nm GaAs pHEMT	40	combined	2	37.9	17	9
[98]	2012	150 nm GaAs pHEMT	17–35	combined	1	22.5	30	10
[12]	2007	500 nm InP DHB T	38	cascode combined	2	30.6	28.6	15
[106]	2008	InP DHB T	20	combined	2	32	37.8	17
[17]	2007	130 nm SiGe BiCMOS	25–40	balanced	2	17	5	10
[15]	2016	180 nm SiGe HBT	20–28	combined	2	29.5	13	-
[18]	2018	130 nm SiGe BiCMOS	12–40	distributed	4 <sup>a</sup>	19	8	-
[99]	2014	100 nm GaN HEMT	6–37	distributed	5 <sup>b</sup>	30	7	10
[23]	2015	200 nm GaN/SiC HEMT	26–30	combined	2	45.5	32	22
[22]	2018	100 nm GaN/Si HEMT	37–43	combined	3	40	23	18
[26]	2019	100 nm GaN/SiC HEMT	26–35	combined	3	37.8	-	22
[107]	2016	28 nm bulk CMOS	28	stacked	2	19.8	43	13.6
[108]	2018	90 nm CMOS	22–30	cascode combined	1	25	27	15
[109]	2020	45 nm CMOS SOI	24–40	differential cascode	2	19	36.6	12

<sup>a</sup>Distributed amplifier with 4 cells, each consisting of a cascode structure with one additional stacked transistor.

<sup>b</sup>Two cascaded distributed amplifiers with 5 cells each.

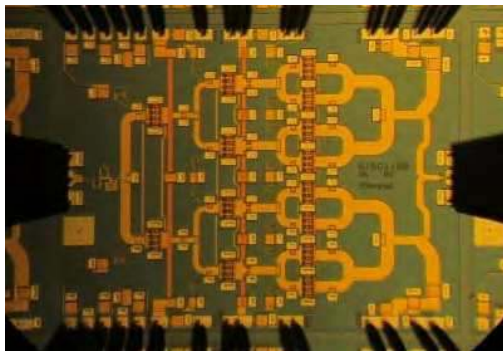


Fig. 15. Broadband 3-stage combined PA in 100 nm GaN/Si [22] ©IEEE 2018.

non-isolating 8-way combiner proposed in [110] attempts to mitigate this detrimental effect thanks to the load modulation occurring when a number of the digitally-controlled transistor cells in the array are turned off. Despite this complex strategy, which is limited to a static turn on/off of the power cells, the resulting PAE at 6 dB OBO remains limited to few percents. A major improvement in the efficiency achievable by CMOS PAs is marked by the recent work of [109], based on a compensated distributed-balun output network. It features a record 19 dBm saturated output power and corresponding PAE in excess of 36% over the range 24–40 GHz, while achieving the highest reported modulation speed (36 Gb/s 64-QAM) among mm-wave PAs below 50 GHz. Notably, the PAE at 6 dB back-off is higher than 10% over the whole bandwidth.

Another recent work where good efficiency is achieved, while targeting high linearity over a wide instantaneous bandwidth, is reported in [111]. The differential 3-stage PA is designed in a 65 nm CMOS process and targets the 26.5–29.5 GHz 5G band. It employs a second harmonic control circuit and a low drop-out (LDO) regulator designed to sup-

press the memory effect generated by the non-linear mixing between the envelope and the fundamental. In CW operation, it achieves 14 dBm saturated power with a corresponding PAE of 20%, and a 22 dB small-signal gain. Remarkably, the third order intermodulation products are maintained under -30 dBc across 1 GHz bandwidth at an output power of 5 dBm.

The state of the art in terms of output power, efficiency and bandwidth for the PAs in the various analysed technologies is reported in Table III.

### B. Doherty PAs

The Doherty PA is a well-established back-off efficiency enhancement technique based on the load modulation principle [112], [113]. While it is widely and successfully applied at communications frequencies (sub-6 GHz), its exploitation for mm-wave bands is still at research level. This is especially critical for CMOS, where complex power combining strategies are typically required to reach the target power levels. On the other hand, the larger power densities of compound semiconductor technologies lead to simpler cells (no need of stacking/combining), thus allowing to exploit more complex topologies.

Around 2000, led by two factors, i.e. the III-V technology improvements and the introduction of complex modulation schemes for backhaul and satellite applications, the necessity and possibility for the first mm-wave MMIC Doherty PAs arose. In 1999, TriQuint [114] presented the first 17 GHz MMIC Doherty PA adopting a 250 nm GaAs process. Two single devices are employed as shown in Fig. 16 to provide 25 dBm output power with a PAE in excess of 40% and a 8 dB small-signal gain. In 2000, the first demonstration of a 20 GHz Doherty PA was given in [115]. It adopts a 150 nm GaAs pHEMT process and achieves similar performance to [114], namely 23 dBm output power, 32% PAE and 8.4 dB small-signal gain. These first works kept at a minimum the stage complexity, without inserting power combiners or driver

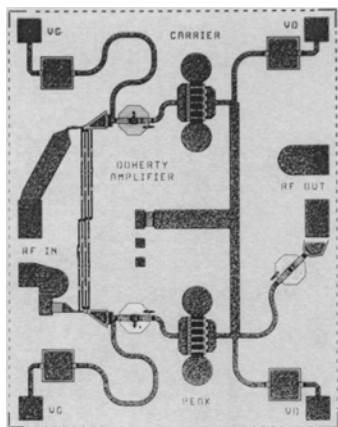


Fig. 16. First Ku-band MMIC Doherty power amplifier in 250 nm GaAs [114] ©IEEE 1999.

stages, leading to limited gain and output power levels. The promising back-off efficiency, higher than 20% at 6 dB OBO in both cases, demonstrated the feasibility of the Doherty concept at Ku- and K-bands, at least for narrowband operation. To develop these initial proofs-of-concept into amplifiers with gain and power levels compatible with the real-field applications, an advancement in the technology was required. At the same time, no strong push from the market existed yet. Around ten years later, these two conditions were verified and brought to multi-stage wideband K-band DPAs.

GaN technology reached the required maturity to develop wideband K-band DPAs around 2012, when TriQuint presented a 37 dBm two-stage DPA adopting 150 nm GaN/SiC HEMTs in the 21–24 GHz band [24]. Although the technology was still under development, this prototype showed very promising performance, achieving higher output power compared to the more mature GaAs technology without the need of power combining, thanks to the higher power density of GaN as well as the better thermal management of SiC substrates. Furthermore, from the design point of view, GaN devices present more favourable impedance levels allowing for simpler matching networks with lower losses and potentially wider bandwidth [116]. As a result, this preliminary example already showed a peak PAE higher than 42% over the whole bandwidth and in excess of 30% at 6 dB OBO at 23 GHz.

In [117] a two-stage Doherty adopting the TriQuint 150 nm GaAs is presented in the band 22.8–25.2 GHz for backhaul applications. The MMIC is one of the first GaAs DPAs in which drivers are embedded in both main and auxiliary branches of the Doherty configuration, as shown in Fig. 18. The paper clearly demonstrates that the position of the driver (in front of the Doherty stage (a) or inside each branch (b)) has a significant impact on the overall PAE, as reported in Fig. 17. In particular, a two-stage DPA in which the drivers are embedded within the Doherty architecture (b) shows a better PAE compared to the case where a single driver feeds the Doherty power stage (a), regardless of the driver efficiency. Moreover, even drivers with limited efficiency (around 20% in this case) are able to improve the PAE compared to the single-stage DPA, besides increasing the gain. On the other

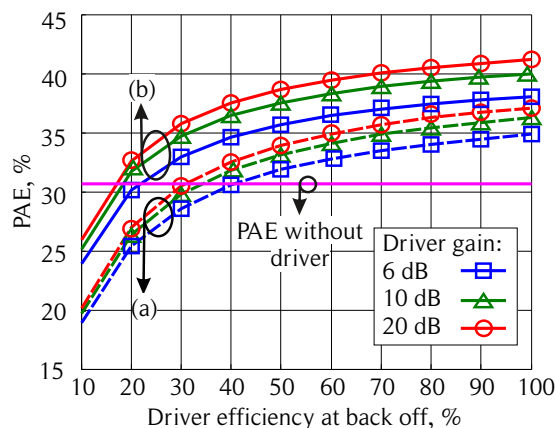


Fig. 17. Study of the impact of the position of the driver in a two-stage Doherty PA from [117]. Simulated total PAE of the two-stage DPA versus driver efficiency for different driver gains. Strategy (a): dashed lines. Strategy (b): solid lines. Ideal DPA PAE without driver: solid horizontal line ©IEEE 2014.

side, the design of the interstage matching networks between the drivers and the power stage is critical, especially when wideband operation is targeted, due to their effect on the signal de-phasing among the branches, which is a key aspect of the DPA operation. In this work no power combining at device level is implemented, but the device periphery of the final stage is significant.

Another work that aims at assessing the feasibility of the Doherty architecture in GaN towards mm-wave frequencies was reported in 2017 [118]. Because at that time the 150 nm GaN technology was not openly available, this work pushes the more stable 250 nm GaN/SiC UMS process at its limits realizing a single-stage 14–15 GHz Doherty PA for point-to-point radio applications. The resulting gain is clearly limited, but the efficiency is comparable to that achieved by state-of-the-art GaAs DPAs (both in saturation and in back-off) with an output power which is four times higher.

In the last few years, the 5G application of the 28 GHz band has given momentum to several new DPA contributions at research level. The two possible scenarios foreseen for 5G active antenna arrays, introduced in Sec. II-C, will require power levels of the order of 30–40 dBm for analog beam-forming and 10–20 dBm in the case of digital beam-forming for the single PA, thus making III-V compounds and Si tech-

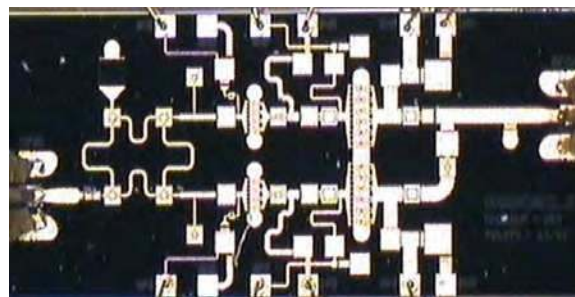


Fig. 18. Two-stage 150 nm GaAs Doherty PA [117] ©IEEE 2014.

TABLE IV  
SOA K-BANDS DOHERTY PAs.

Ref.	Year	Technology	Freq. (GHz)	Final stage topology	N. of stages	$P_{SAT}$ (dBm)	$PAE_{SAT}$ (%)	$PAE_{OBO}^a$ (%)	SS Gain (dB)
[117]	2014	150 nm GaAs pHEMT	22.8–25.2	single device	2	29.9	25	14	11
[119]	2017	150 nm GaAs pHEMT	29.25–30.25	single device	2	27	35	28	10
[120]	2018	150 nm GaAs pHEMTs	29–31.8	single device	2	25.7	31	21 <sup>b</sup>	12
[121]	2018	150 nm GaAs pHEMTs	27.25–28.5	combined stacked	2	28	34	24	13
[122]	2019	150 nm GaAs pHEMTs	26.5–29.5	combined	2	25	35	25	10
[24]	2012	150 nm GaN/SiC HEMT	21–24	single device	2	37	42	-	-
[123]	2019	100 nm GaN/Si HEMT	27.5–28.35	single device	2	32	25	28	10
[31]	2018	45 nm CMOS SOI	25–31	stacked	1	20	30	20	10
[30]	2019	45 nm CMOS SOI	27	cascode, mixed-signal	2	23.3	40.1	33.1	19.1
[20]	2019	130 nm SiGe BiCMOS	29–31	differential	2	16.8	20.3	13.9	15
[21]	2020	130 nm SiGe BiCMOS	24–30	differential	2	28	30	20	20

<sup>a</sup>PAE at 6 dB OBO, unless otherwise noted.

<sup>b</sup>PAE at 7 dB OBO.

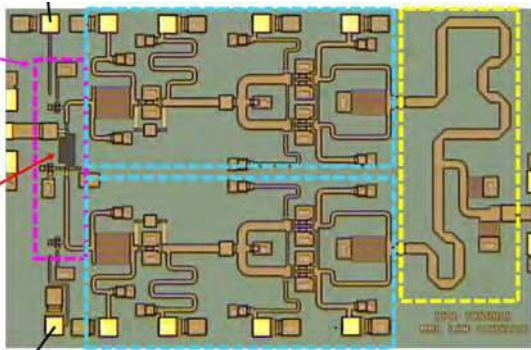


Fig. 19. Two-stage Doherty in 150 nm GaAs adopting a combined final stage [122] ©IEEE 2019.

nology, respectively, the most appropriate choice. As a result, seed contributions in the mature and reliable GaAs technology [119]–[122] appeared, which are two-stage Doherty MMICs achieving output power of the order of 25 dBm and linear gain in excess of 10 dB over bandwidths wider than 1 GHz. The PAE achieved in saturation ranges from 30 to 35%, while the PAE at 6 dB output back-off results clearly much higher than the classical counterparts (20–30%, versus 10–15%), paving the way to the exploitation of those techniques for future commercial 5G-NR. In these works, power combining at device level starts to appear in the power stage, either as simple parallel combination in [122] (Fig. 19) or with the further addition of device stacking in [121] (Fig. 20), to reach the required total power expected from the single PA, easier adopting GaN.

One of the first examples of GaN DPA for 5G-NR has been recently presented in [123], and based on a GaN on Si technology. In the band 27.5–28.35 GHz, it shows 32 dBm output power, 25% saturated PAE and 28% back-off PAE. In this work, the advantages of GaN in terms of power density are not yet completely exploited due to the partial immaturity of the technology but the back-off efficiency is already promising, suggesting that in a short while the technology improvement will lead to interesting results.

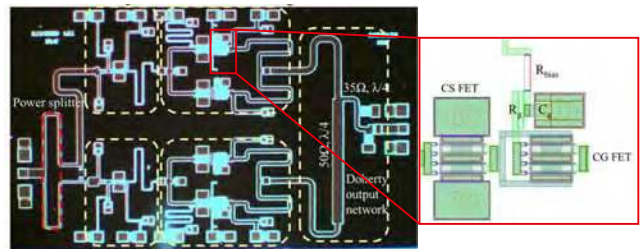


Fig. 20. Two-stage Doherty in 150 nm GaAs combining two 2-stacked cells in the final stage [121] ©IEEE 2018.

During the same years, Si-based DPAs (CMOS and SiGe BiCMOS) have become feasible for the 5G digital beam-forming scenario [19], [20], [30], [31], which requires power levels (10–20 dBm) low enough to be reached by low-complexity power combining structures. Until recently, the record bandwidth (> 5 GHz) belonged to CMOS PAs [31], with a resulting efficiency on the average comparable or lower than their compounds counterparts. On the other side, DPAs have much higher back-off efficiency than the standard PAs presented in Sec. IV-A in the same technology. Finally, a very recent 2-stage DPA in 130 nm SiGe BiCMOS is presented in [21], achieving 28 dBm saturated power, 30% peak PAE, and 20% PAE at 6 dB back-off from 24 GHz to 30 GHz. This represents the SoA output power among 28 GHz SiGe/CMOS K-bands PAs, effectively competing with compounds DPAs in terms of both output power and efficiency.

To complete the K-bands scenario, two other technologies that have been exploited at the early stages are the GaAs mHEMTs and InP-based devices. Both have been tested when the other technologies were still unable to provide the required power or gain, but they are now less researched.

One of the first examples of InP PA in K-band was presented in 1994 [124], with the state-of-the-art performance of 28 dBm output power and 31% PAE at 44.5 GHz. After the advent of the double heterojunction structure, several examples became



available, such as [12], [106] which achieved output power in excess of 30 dBm with peak PAE higher than 30%. It progressively disappeared after 2010, moving to higher frequencies, mainly due to its high production costs, as shortly mentioned in Sec. II.

GaAs mHEMTs have also been used to take advantage of the higher gain of such technology. The first multi-watt mHEMT PA was presented by BAE Systems in [104], which demonstrated 35 dBm output power, 39% PAE and 24 dB linear gain with only two stages. A very wide bandwidth PA for radar applications is reported in [105]. It adopts a two-stage configuration where parallel resistive feedback is used to provide a flat gain response and to reduce the sensitivity to process variations. It achieves 20 dB of small-signal gain and around 10 dBm output power from 18 to 40 GHz.

The state of the art DPAs in K-bands are summarised in Table IV.

### V. V-BAND (40–75 GHz)

The 40–75 GHz spectrum, commonly known as the “V-band” [125], is one of the most widely exploited mm-wave bands for high capacity mm-wave communications. Like other mm-wave bands, V-band wireless links also require unobstructed line-of-sight channels and exhibit considerable path loss that demands high antenna gain for compensation. In addition to the significant rain fade effect in V-band [126], it is noteworthy that the atmospheric oxygen absorption peaks at 60 GHz with a sea-level attenuation of 20 dB/km [125]. As a result, the V-band spectrum is primarily used for high-capacity and short-distance (less than 2 kilometres) communications. Over the 57–71 GHz FCC unlicensed band, the WiGig or IEEE 802.11ad standard was announced in 2009 with up-to six contiguous 2.16 GHz-channels, targeting applications like wireless transmission of uncompressed UHD videos with up-to 7 Gbit/s over 10 meters [127]. Following that, IEEE 802.11ay is proposed as the next-generation 60 GHz WiFi and the second WiGig standard. It supports a maximum bandwidth of 8.64 GHz by carrier aggregation/bonding as well as multi-stream MU-MIMO for up-to 100 Gb/s and 300–500 meters of extended range for various applications, including mm-wave backhaul, fixed wireless access for homes/businesses [128]. In addition, the 37–50 GHz spectrum is proposed for the next-generation communication for non-geostationary satellite constellations.

These high-data-rate high-capacity communication applications largely drive the design of V-band power amplifiers, necessitating a balanced performance of output power, bandwidth, linearity, and energy efficiency. For compound semiconductor PAs, GaAs is a very popular technology of choice for V-band PAs. In the 40–50 GHz sub-band, the best reported GaAs PA achieves a saturated power in excess of 34.5 dBm with peak PAE of around 25% and 13 dB power gain at 45 GHz [129]. To connect power devices with large output peripheries, [129] uses a transmission-line (T-line) based in-phase combiner on four PA cells, as shown in Fig. 21, with lower passive loss compared to a conventional Wilkinson combiner. In the range 60–75 GHz, reported GaAs PAs support

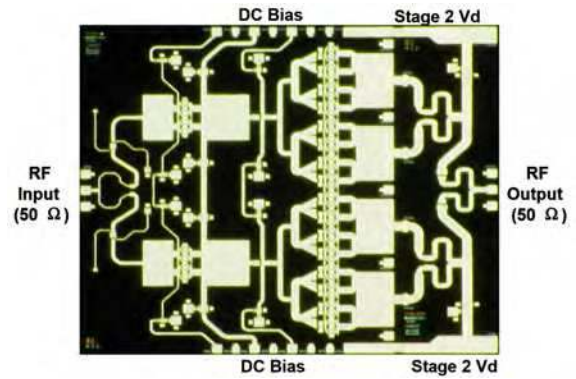


Fig. 21. GaAs pHEMT PA at 44.5 GHz [129] ©IEEE 2005.

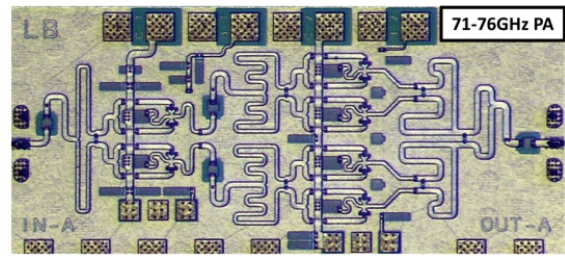


Fig. 22. InP HBT PA at 71–76 GHz [134] ©IEEE 2015.

32.5 dBm saturated power and 25 dB gain at 60 GHz [130], and saturated power higher than 28 dBm and 26 dB power gain from 71 to 76 GHz [131]. T-line power combiners are extensively used in these high power PAs.

GaN has also been widely employed for V-band PAs. The recent PA in [22] that covers the upper portion of Ka-band and the lower portion of V-band, which has already been presented in Sec. IV (Fig. 15), shows remarkable performance. The PA in [132] realizes 33 dBm saturated power with 24.6% peak PAE and 12 dB power gain over the 70–86 GHz sub-band, covering both the up-link (71–76 GHz) and down-link (81–86 GHz) satellite communication bands.

Various InP technologies have been used for V-band PA designs targeting medium-power but high-efficiency applications. The PA in [124] uses InP HEMT technology and pushes the output power to 28 dBm at 44.5 GHz with a high PAE of 31%. At 60 GHz, an InP HEMT PA supports 23.5 dBm output with 43% PAE [133], which is also the highest reported PAE. At 71–76 GHz, the InP HBT PA shown in Fig. 22 realizes 26 dBm output power, 23% PAE and 10 dB gain [134]. It combines four output PA cells, each of which is formed by two multi-finger InP devices and output passive network that can carry high DC biasing current.

The increasing need for medium-power PAs to address array-based high-capacity short-range applications also stimulates the research and development on silicon-based V-band PAs. At upper V-band frequencies (60–75 GHz), advanced silicon processes still offer adequate power gain (e.g.,  $f_{MAX}$  of 350 GHz for Globalfoundries 45 nm CMOS SOI), while distributed passives and antennas become commensurate with

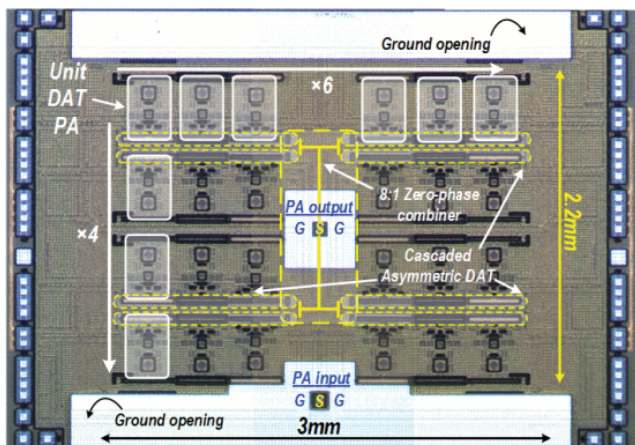


Fig. 23. 60 GHz PA in 45nm CMOS SOI using asymmetric coupler DAT combining [135] ©IEEE 2019.

on-chip active circuits due to the reduced signal wavelength; this interesting combination has opened the door to a plethora of design innovations.

Boosting the output power of silicon PAs at this frequency is of a primary interest to ensure sufficient link budget and coverage. The on-chip passive power combiner is therefore often a key focus in V-band PA designs. The major consideration is how to best manage the impedance transformation, passive loss, and bandwidth of on-chip passive power combiners. Similar to lower frequency PAs, on-chip transformers are popular choices for medium-power applications ( $\sim 20$  dBm) with a compact form-factor [69]. To achieve even higher output power, the combiner's scalability becomes critical, and on-chip T-line combiners are demonstrated for 60 GHz and above [136], [137]. In particular, [136] reports a 16-way T-line power combiner on 3-stage single-ended PA cores in 90 nm SiGe which achieves 27.3 dBm saturated power, 22.3 dBm power at 1 dB compression and 12.4% PAE with a 1.8 V supply. There are also explorations on the distributed active transformer (DAT) for series power combining that is especially useful for PAs using low-voltage silicon devices [138], [139]. However, using transformer magnetic coupling for DAT combiners fundamentally needs "circular-shape" output arrangement and results in substantially complicated input signal distribution, low area-efficiency, and limited scalability on the number of combining paths. Recently, a 60 GHz PA using an asymmetric coupler-based series power combiner is proposed and demonstrated [135] in 45 nm CMOS SOI process (Fig. 23). Cascading asymmetric couplers achieve DAT-based power combining by providing equal load impedance on identical sub-PA. The coupler structure also supports differential PA cores with broadband capacitive neutralization for higher PA core gain, stability, and output power. Moreover, this architecture achieves DAT-based series power combining with a "line-shaped" non-circular layout, and multiple coupler-based DAT PAs can be further power combined using zero-degree T-line combiner, essentially as hybrid series-parallel combining, to boost the PA output power. This 60 GHz CMOS SOI PA realizes on-chip power combining of 24 sub-PAs and

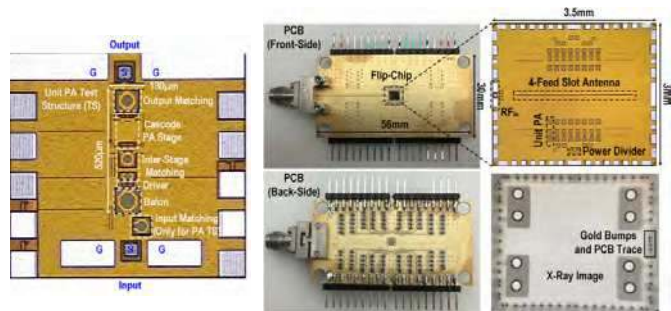


Fig. 24. 60 GHz unit-PA (left) and multi-feed radiator (right) in 45 nm CMOS SOI for on-antenna power combining [141] ©IEEE 2017.

achieves 30.1 dBm output power, 24.7 dB power gain, and 20.8% peak PAE, as well as 12 Gb/s 64-QAM and 8 Gb/s 16-QAM modulations with long-term reliability, leading the state of the art of high-power V-band PAs.

Besides power combiners, there is also extensive research on stacking Si PA devices to sustain a high supply voltage with minimum impedance transformation for high output power. Unlike conventional cascode PAs, stacked transistor PAs require appropriate voltage swings at the gate/base terminals of the stacked devices to ensure reliability [71], [110], [140]. In addition to reliability, managing the amplitude and phase of these gate/base voltage swings is highly critical yet non-trivial at V-band, which often limits the achievable PA efficiency and linearity in practice. The stacked PA topology has been explored in both SiGe and CMOS SOI technologies, with the CMOS SOI particularly conducive to stacking more devices due to the floating body. Moreover, stacked PAs have been reported for both class-AB linear PAs and quasi-switching class-E PAs for further efficiency enhancement.

Another technology direction is to improve the PA bandwidth and intrinsic linearity. Such broadband linear medium-power PAs are critical components for large-array systems with massive spatial power combining [65], [142], [143]. Like broadband PAs at lower frequency [53], high-order passive networks are typically used to provide a large-signal optimum load to the power devices over a wide frequency range [142]. For PA linearity, static biasing and dynamic biasing can be optimized to ensure flat AM-AM linearity. In CMOS PAs, using NMOS and PMOS to compensate for the device AM-PM nonlinearity has been a common practice, while for multi-stage PAs, using drivers and output stages for nonlinearity compensation is also widely exercised [144], [145].

There are also increasing explorations of boosting the back-off efficiency for V-band PAs. This is essential for high capacity wireless communication that support complex and spectrally efficient modulations with large PAPR. Reported approaches include Doherty PAs, Outphasing PAs, and an asymmetrical non-isolating combiner PA [143]. However, due to the high loss in passive networks and degraded active devices, e.g., gain, efficiency, and output impedance, most of these V-band PAs show very limited back-off efficiency enhancement compared to class-B PA operations and often exhibit degraded linearity, requiring extensive digital pre-



TABLE V  
SOA V-BANDS PAS.

Ref.	Year	Technology	Freq. (GHz)	Topology	N. of stages	$P_{SAT}$ (dBm)	$PAE_{SAT}$ (%)	SS Gain (dB)
[129]	2005	150 nm GaAs pHEMT	45	4-way combined	2	34.5	25	13
[130]	2005	150 nm GaAs pHEMT	60	8-way combined	2	32.5	-	25
[131]	2015	100 nm GaAs pHEMT	71–76	8-way combined	4	28	13	26
[132]	2018	70 nm GaN HEMT	70–86	8-way combined	4	30	8	16
[124]	1994	150 nm InP HEMT	44.5	single-stage	1	28	31	7
[134]	2015	150 nm InP HEMT	71–76	4-way combined	2	26	23	10
[136]	2016	90 nm SiGe	68–91	16-way combined	3	27.3	12.4	19.3
[142]	2014	28 nm bulk CMOS LP	40–67	differential	2	13	16	13
[135]	2019	45 nm CMOS SOI	56–63	24-way combined	3	28.5	15	24
[146]	2019	45 nm CMOS SOI	60	differential Doherty	3	20.1	26 <sup>a</sup>	13

<sup>a</sup>and 16.6% PAE at 7 dB OBO.

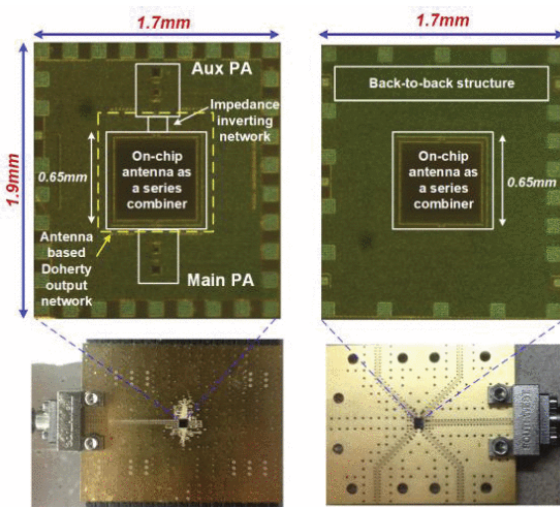


Fig. 25. 60 GHz multi-feed radiator in 45 nm CMOS SOI for on-antenna Doherty active load modulation and power combining [147] ©IEEE 2019.

distortion (DPD) in practice. A recent 60 GHz Doherty PA in 45 nm CMOS SOI uses on-chip coupler baluns to construct a low-loss Doherty load modulation network [146]. It measures 20.1 dBm saturated power and 26% PAE, as well as 16.6% PAE at 7 dB back-off with  $1.45\times$  PAE enhancement over a class-B PA, presently leading the V-band PAs with back-off efficiency enhancement.

Recently, there is a new trend on mm-wave frontend innovations that merges antennas together with frontend electronics to achieve both desired radiations and various new “on-antenna” functionalities. For example, antennas can be designed and driven by multiple electronics paths as “multi-feed antennas” (Fig. 24). It is shown that multi-feed antennas can achieve on-antenna power combining and inherent impedance transformation among the feeds before using any on-chip passive networks, which greatly improves the combining efficiency over conventional on-chip passive combiners. A 4-feed on-chip slot antenna is demonstrated to realize parallel power combining of total 16 sub-PAs at 60 GHz and achieve 27.9 dBm saturated power and 23.4% PAE on a 45 nm CMOS SOI process [141]. A near-field coupled slot antenna

array achieves power combining of 8 sub-PAs for 27.4 dBm saturated power and 30.8% drain efficiency at 74 GHz in a 65 nm bulk CMOS process [148]. Moreover, multi-feed antennas serve as part of the Doherty or outphasing active load modulation network [147], [149], [150] (Fig. 25). [147] shows a 2-way Doherty radiator using a dual-feed on-chip loop antenna at 65 GHz, achieving 19.4 dBm saturated power and PAE of 28.3% and 20.1% at saturation and 6 dB back-off, realizing  $1.46\times$  PAE enhancement at 6 dB back-off over an ideal class-B PA. [149] shows that two near-field coupled multi-feed slot antennas realizes a 3-way Doherty radiator with 21.2 dBm saturated power, 20.7 dBm power at 1 dB compression, and PAE of 21.8%/20.6%/20.1%/19.3% at  $P_{sat}/OP1dB/4dB-PBO/8dB-PBO$ , achieving  $1.42\times$  and  $2.34\times$  PAE enhancement at 4 dB-PBO and 8 dB-PBO over an ideal class-B PA. Both Doherty radiators/PAs realize the best back-off efficiency enhancement among reported V-band PAs. Moreover, compared to spatial polar combining with a very limited field-of-view (FoV) [151], both Doherty radiators/PAs first combine the output power of main and auxiliary paths before radiating it out, which supports full antenna FoV (beyond  $-45^\circ$  to  $+45^\circ$ ) with multi-Gbit/s 64-QAM and 16-QAM modulations and no DPD.

The state of the art in terms of output power, efficiency and bandwidth for the various technologies previously mentioned is reported in Table V.

## VI. W-BAND (75–110 GHz)

W-band frequency spectrum (75–110 GHz) has been deployed in a number of applications thanks to its low atmospheric attenuation and the capability of providing high data rate throughput. In particular, the 77 GHz band is used for automotive cruise control radars. The 94 GHz window is widely employed in mm-wave imaging applications, including defense, astronomy, and security systems. More importantly, the 71–76 GHz and 81–86 GHz segments are allocated for satellite services and long-haul transmission [152]. As the low-frequency spectrum becomes more crowded and suffers from orbit congestion, W-band satellite systems have recently gained much interest from research and industry. Furthermore, the recent 5G development has pushed the frequency of many applications such as automotive radars, long-haul optical

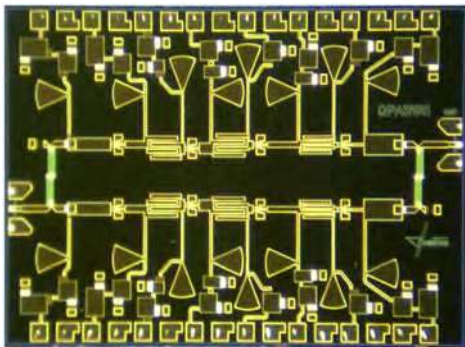


Fig. 26. Four-stage balanced GaAs MMIC amplifier ( $2.7 \times 1.85 \text{ mm}^2$ ) [154] ©IEEE 2012.

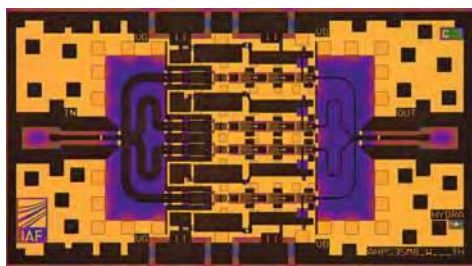


Fig. 27. 65–125 GHz Stacked-FET GaAs MMIC PA ( $1.75 \times 1 \text{ mm}^2$ ) [156] ©IEEE 2018.

communications, and measurement instrumentations into the W-band spectrum [153]. One of the biggest challenges in solid-state W-band power amplifiers is the ability to provide high power with good efficiency. The difficulty is mainly due to the limitation of the semiconductor processes. Within the same semiconductor technology, the breakdown voltage of the transistors is typically reduced when the cut-off frequency  $f_T$  increases. Moreover, high passive losses at W-band significantly degrade the amplifier efficiency. Nonetheless, in the past decades, W-band PAs have been demonstrated in various technologies: GaAs, GaN, InP, SiGe, and CMOS.

The very first W-band amplifiers were designed in GaAs and InP processes around the early 90s. In 1990, Advantek introduced the first single-chip GaAs amplifier operating from 85 to 95 GHz [155]. The work presented two circuits using a sub 200 nm MESFET and pHEMT devices with an  $f_T$  of 100 GHz and  $f_{MAX}$  of 200 GHz. Although the gain was still low, and efficiency was not reported due to measurement capability, the works laid out a solid foundation for W-band power amplifier design. The 0.1- $\mu\text{m}$  GaAs T-gate technology, which was first developed by TRW Inc., is the most popular GaAs technology deployed in W-band. Using this T-gate technology, multi-stage amplifiers have been reported. Among these, the push-pull amplifier presented in 1995 in [63] achieved a record (at that time) 13 dB small-signal gain and 13.3% PAE at 18.8 dBm at 90 GHz. Most W-band power amplifiers reported in the 90s mainly focused on the 94 GHz band for military radar applications. Other frequencies in W-band have been later explored for automotive radar at 77 GHz [157], broadband mm-wave imaging 72–95 GHz [158], and the far-infrared

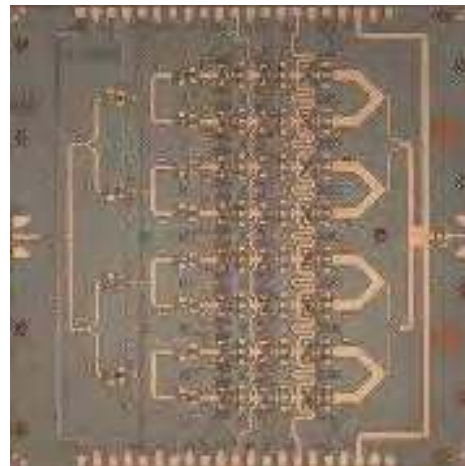


Fig. 28. Five-stage 92–102 GHz GaAs MMIC PA ( $3 \times 3 \text{ mm}^2$ ) [161] ©IEEE 2018.

and sub-millimeter telescope [159]. In particular, the authors in [159] demonstrate three amplifier modules that cover three different sub-bands: 72–81, 90–101, and 100–113 GHz. Regarding wideband applications, Fig. 26 presents a fully integrated MMIC that covers that whole W-band from 75 to 100 GHz [154]. The single chip can provide an average of 14.5 dBm output power across the entire bandwidth. Four identical MMICs in Fig. 26 are then combined using a 4-way septum power combiner to achieve up to 20 dBm output power with an associated gain of 15 dB over 75–110 GHz. Recently, an ultra-wideband amplifier has been presented in a 50 nm InAlAs/InGaAs mHEMT technology developed by Fraunhofer IAF with an  $f_T$  of 375 GHz and  $f_{MAX}$  of 670 GHz [156]. The schematic and chip photo of the  $1.75 \times 1 \text{ mm}^2$  MMIC amplifier based on stacked-FET unit cells are illustrated in Fig. 27. The prototype achieves 22 dBm output power, 16.8 dB small-signal gain, and a peak PAE of 10.7%. Most notably, the bandwidth is extended beyond W-band, covering from 65 to 125 GHz. Using a 0.1- $\mu\text{m}$  GaAs pHEMT process with solder hot-via RF transition, the authors in [160] demonstrate a 28 dBm output power and a 22 dB small-signal gain from 81–86 GHz, which is the highest output power achieved by a single GaAs MMIC in W-band to date. Fig. 28 presents a 5-stage MMIC that exhibits a 27 dBm maximum power and 27 dB of gain from 92–102 GHz [161]. The measured 12.5% peak PAE is the highest PAE reported above 100 GHz using GaAs technologies.

Besides GaAs, InP HEMT and HBT processes have also been deployed in W-band PAs since the early 90s. In 1991, an InP MMIC presented by Device Laboratory using a 0.1- $\mu\text{m}$  T-gate InP HEMT process achieves a maximum gain of 12 dB, and the bandwidth covers from 75 to 100 GHz [163]. As compared to GaAs, InP technologies generally provide slightly lower output power, but at higher efficiency. 20% PAE with an associated 26.3 dBm output power recorded in [164] is among the highest power reported to date using InP processes at W-band. Furthermore, using a 0.1- $\mu\text{m}$  HEMT process, a finite-ground coplanar waveguide design, which



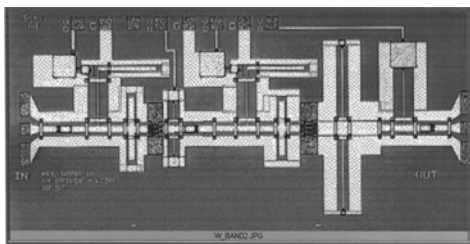


Fig. 29. Two-stage W-band finite-ground-coplanar-waveguide InP MMIC PA ( $2.4 \times 1.1 \text{ mm}^2$ ) [14] ©IEEE 1999.



Fig. 30. W-band PA using a 250-nm InP DHBT ( $1.08 \times 0.68 \text{ mm}^2$ ) [162] ©IEEE 2017.

is shown in Fig. 29, exhibits an 18.2% PAE with 18.6 dBm output power and 14.3 dB gain at 94 GHz [14]. Recently, double heterojunction bipolar transistor (DHBT) technology, which has the advantage of providing better linearity and efficiency over HEMT devices, has become more popular among InP processes. Most notably, Northrop Grumman Corporation presents an InP MMIC amplifier using an advanced 250 nm InP DHBT [162]. As shown in Fig. 30, the work reports a remarkable 41.7% PAE with a saturated power of 12.4 dBm at 93 GHz, which is the highest efficiency W-band PA reported in open literature.

Although recent development in GaAs and InP technologies provides a great enhancement in power, bandwidth, and efficiency in W-band PAs, the maximum output power of a single MMIC is still limit below 1W. To achieve watt level performance at W-band, GaN MMIC is the only candidate. High-frequency GaN on SiC processes have been developed by HRL Lab since 2006 with the first W-band three-stage GaN MMIC reporting 25 dBm output power with 14% PAE at 80.5 GHz [165]. Recently, Fujitsu developed an 80 nm GaN HEMT process that observes among the highest power density of 3.6W/mm at W-band [166]. A  $2 \times 1.8 \text{ mm}^2$  MMIC shows a measured output power of 30.6 dBm with a small-signal gain of 18.9 dB and a peak PAE of 12.3% at 86 GHz. One of the most advanced GaN processes is the 40 nm T-gate process developed by HRL Lab which has an  $f_T$  of 200 GHz and  $f_{MAX}$  of 400 GHz with the breakdown voltage up to 40 V. The fabricated prototype achieves over 20 dB gain from 79–95 GHz, an output power of 31.3 dBm at 27% PAE [27]. In addition to conventional reactive matching amplifiers, several techniques have been introduced in GaN MMIC PAs to extend the bandwidth. For instance, Fig. 31 shows a traveling-wave three-stage GaN amplifier presented

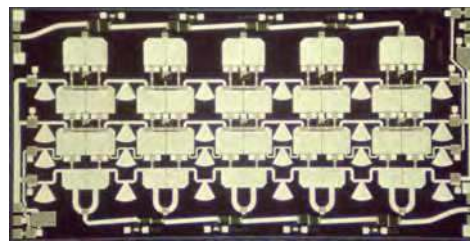


Fig. 31. Broadband traveling wave W-band GaN MMIC ( $2.75 \times 5.4 \text{ mm}^2$ ) [167] ©IEEE 2015.

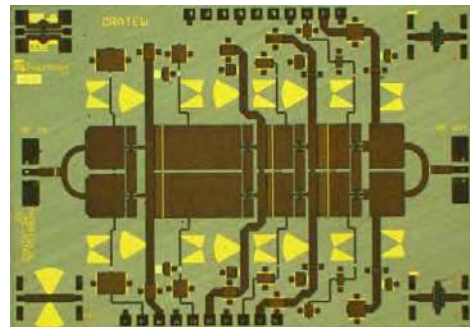


Fig. 32. Four-stage broadband radial stub MMIC [168] ©IEEE 2018.

by Quinstar in [167] achieves more than 33 dBm power and at least 16 dB gain from 75 to 100 GHz. On the other hand, in [168], a broadband radial stub is deployed in a W-band PA using a 100 nm Fraunhofer IAF GaN HEMT process to cover the completed W-band from 70 to 110 GHz. The MMIC in Fig. 32 demonstrates a maximum power and gain of 28.6 dBm and 8.6 dB, respectively. Higher output power can also be achieved by employing off-chip waveguide combiners. For instance, an outstanding high power 45.6 dBm GaN amplifier module has been demonstrated from 75 to 100 GHz using septum combiners and 12-way radial combiners [22] [169].

Despite the capability to provide high output power over a wide frequency range, GaAs and GaN MMICs typically consume a large amount of dc power, have large chip size, and low level of integration. On the other hand, Silicon-based circuits, which have been dominated in commercial applications at RF frequencies thanks to their high level of integration and low cost, are more suitable for applications requiring below 20 dBm power. In particular, the 65 nm and

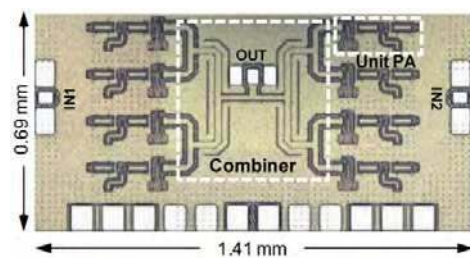


Fig. 33. 45 nm SOI CMOS W-band amplifier using 8-way zero-degree combiner ( $0.69 \times 1.41 \text{ mm}^2$ ) [170] ©IEEE 2014.



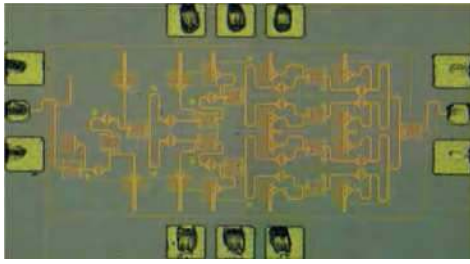


Fig. 34. 77–110 GHz power amplifier in 65 nm CMOS process ( $0.95 \times 0.6 \text{ mm}^2$ ) [171] ©IEEE 2014.

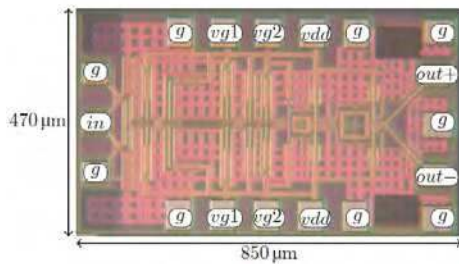


Fig. 35. 76–106 GHz power amplifier in 40 nm CMOS process ( $0.85 \times 0.47 \text{ mm}^2$ ) [175] ©IEEE 2016.

45 nm CMOS processes prove themselves to be better candidates for high gain and high efficiency W-band amplifiers. In particular, the authors in [172] present a 65 nm CMOS amplifier that exhibits a measured output power of 19.3 dBm with a gain of 24.2 dB and peak PAE of 19.2%. To overcome the low breakdown limitation of CMOS processes, stacked-FET is utilized in [173] to provide 19 dBm at 90 GHz. Fig. 33 presents a 45 nm SOI CMOS W-band amplifier using an 8-way zero-degree combiner [170]. The circuit achieves a maximum output power of 21.1 dBm with a gain of 10 dB. However, the peak PAE is only 5.2% due to the high losses from the power combiner. To minimize the losses, a broadband parallel-series power combiner is employed in a 40 nm CMOS PAs [174]. The PA biased at 0.9 V can deliver 20.9 dBm power at 22.3% PAE, which is among the highest PAE reported to data in W-band CMOS PAs. In terms of bandwidth, the full W-band CMOS PA in 65 nm CMOS has been reported in [171]. The MMIC PA shown in Fig. 34 exhibits an 18 dB small-signal gain with the bandwidth covers from 77–110 GHz. Similarly, 40 nm CMOS PA in [175] employs transformers and capacitor coupling as shown in Fig. 35 to achieve 18 dB gain from 76–106 GHz. Nonetheless, the former circuit only has a peak PAE of 4.5% while the latter shows 10% PAE. Spatially power-combined has also been demonstrated on a  $2 \times 4$  SOI CMOS amplifiers array [176]. The total output power recorded is 24 dBm, which is the highest W-band output power from a single CMOS chip reported to date.

SiGe BiCMOS technology provides a good balance solution that can achieve higher breakdown voltage than CMOS processes, utilize the good linearity and efficiency BJT devices while still preserve the high level of integration and maintain a compact chip size.

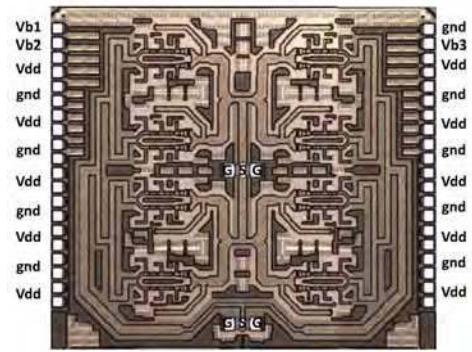


Fig. 36. 90 nm SiGe W-band amplifier using a 16-way combiner ( $2.7 \times 2.4 \text{ mm}^2$ ) [136] ©IEEE 2016.

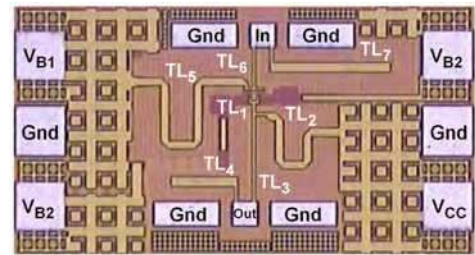


Fig. 37. Class-E SiGe W-band amplifier with 40.4% peak PAE ( $0.9 \times 0.49 \text{ mm}^2$ ) [177] ©IEEE 2015.

A 68–91 GHz PA using an advanced 90 nm 9HP SiGe process from Global Foundries (previously known as IBM) has been demonstrated [136]. The prototype shown in Fig. 36 demonstrates a measured output power of 27.3 dBm with an associated PAE of 12.4% and a small-signal gain of 19.3 dB. The design is the highest power silicon-based W-band PA reported to date. It uses a 16-way T-line power combiner on 3-stage single-ended PA cores in 90 nm SiGe. To achieve high efficiency, the class-E amplifier design is investigated in [31]. The MMIC shown in Fig. 37 demonstrates an outstanding 40.4% PAE at 17.7 dBm output power at 93 GHz. Although the class-E switching technique can provide high PAE performance, the voltage swing typically exceeds the breakdown voltage of the transistor, posing an issue for long-term reliability.

Besides conventional amplifiers and power combining techniques, Doherty amplifiers have also been explored to improve efficiency at back-off power. In [68], the authors present a 40 nm CMOS Doherty amplifier at 77 GHz for base-station backhaul communications. Despite high losses of the silicon substrate, the circuit achieves a peak PAE of 12% at 16.2 dBm output power and a 5.7% PAE at 6-dB power back-off. Table VI summarizes the power, gain and efficiency performances of state-of-the-art W-band PAs using different technologies.

## VII. ABOVE 110 GHz

In this review section, we focus on power amplifier technologies beyond 110 GHz, mostly between 110 GHz and 300 GHz. In this upper mm-wave frequency regime, the short

TABLE VI  
SOA W-BANDS PAS.

Ref.	Year	Technology	Freq. (GHz)	Topology	N. of stages	$P_{SAT}$ (dBm)	$PAE_{SAT}$ (%)	SS Gain (dB)
[156]	2018	50 nm GaAs mHEMT	65–125	stacked	1	22	10.7	16.8
[161]	2018	100 nm GaAs pHEMT	92–102	single-ended	5	27	12.5	27
[164]	1999	150 nm InP HEMT	85–95	single-ended	2	26.3	19	12
[162]	2017	250 nm InP DHBT	93	single-ended	1	12.4	41.7	10
[27]	2014	40 nm GaN HEMT	65–110	single-ended	3	31.1	27	20
[167]	2015	100 nm GaN HEMT	75–100	travelling wave	3	34.7	12.1	16
[169]	2016	100 nm GaN HEMT	75–110	off chip	3	45.7	-	14
[172]	2012	65 nm CMOS	79	8-way combined	4	19.3	19.2	24.2
[174]	2014	40 nm CMOS	71–86	4-way combined	2	20.9	22	18.1
[136]	2016	90 nm SiGe BiCMOS	68–91	16-way combined	3	27.3	12.4	19.3
[177]	2015	130 nm SiGe BiCMOS	93	class-E	2	17.7	40.4	15

wavelength of the electromagnetic waves is attractive for high resolution radar, imaging systems to detect concealed weapons, synthetic aperture radar (SAR) systems to track maneuvering targets and image scenes on the battlefield [40], [178]. One example is the DARPA Video Synthetic Aperture Radar operating at 235 GHz and providing real-time high resolution video SAR imagery [179]. In March 2019, the Federal Communication Commission (FCC) voted to open up 21.2 GHz unlicensed spectrum between 116 GHz and 246 GHz [180]. The frequency bands above 100 GHz can potentially be used for 6G networks and wireless applications.

In this frequency regime, scaled field-plate GaN HEMTs are the leading technology that provides the highest power density and breakdown voltage [33], [181].

The process parameters of the scaled GaN HEMT processes available from HRL Lab [33] are provided in the comparison Table I. In addition to the 40 nm gate length T3 process already mentioned in Sec. VI, the 20 nm T4 process features  $f_T$  and  $f_{MAX}$  of 329 GHz and 558 GHz, respectively.

More importantly, the breakdown voltage of the T4 process is 17 V, which is more than 10 times of those of scaled GaAs, InP, CMOS and SiGe technologies in the same frequency range [182]. Therefore, it is expected that GaN power amplifiers can provide watt-level output power in the frequency regime of 110 to 220 GHz. While GaN HEMT MMICs have been shown to have stellar parameters that are highly favorable for power amplifiers of greater than 30 dBm power beyond 110 GHz, only a few power amplifiers have been reported in open literature. In 2014, the 1st G-band 180–200 GHz GaN MMIC PA reported in [33] only achieves 14 dBm output power with an associated 4.5 dB gain. Recently, a PA at 115 GHz has also been reported using a 100 nm GaN HEMT process from Fraunhofer IAF [183]. The four-stage design achieves a very high gain of 34.8 dB and a maximum power of 20.3 dBm.

The highest output power single die GaN amplifiers that have been reported in literature in 2018 are the 29.5 dBm output power PA from 102 to 118 GHz, and the 27 dBm output power one from 98 to 122 GHz [181]. The two highest output power amplifiers, which are shown in Fig. 38, were designed by Quinstar and fabricated by HRL Laboratories, Malibu, CA using their 150 nm T2 GaN process on a 50  $\mu$ m thick SiC substrate [33], [181]. The T2 process features a double-

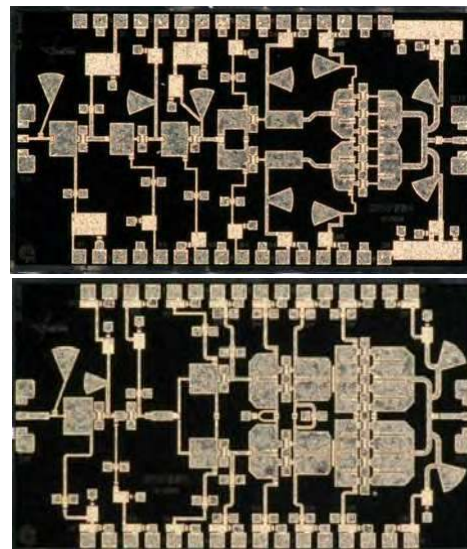


Fig. 38. Five-stage amplifiers in 150 nm T2 GaN process of HRL Laboratories: 27 dBm 98–122 GHz PA (top), and 29.5 dBm 102–118 GHz PA (bottom) [181] ©IEEE 2018.

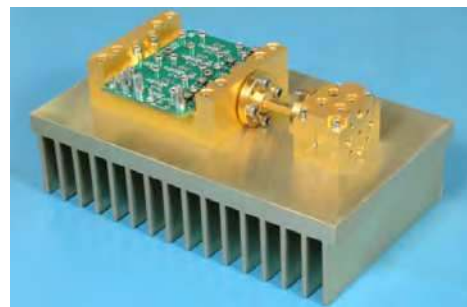


Fig. 39. SSPA module based on the combination of four GaN MMIC power amplifiers in a hybrid assembly with H-tee waveguide combiner [181] ©IEEE 2018.

heterostructure field-effect transistor (DHFET) with a typical  $I_{max}$  of 1 A/mm. The main DHFET used in the final stage has a total gate width of 100  $\mu$ m consisting of four 25  $\mu$ m unite fingers. The 100  $\mu$ m DHFET achieves a measured gain of 8.44 dB at 87 GHz with 12 V drain voltage operation and a



power density of 1.8 W/mm. In order to achieve 20 dB gain, the authors have developed two five-stage power amplifiers (Fig. 38). The second PA has twice the total gate width from stages 3 to 5 to produce higher output power. For instance, the final stage of the 29.5 dBm PA employs eight  $100\ \mu\text{m}$  transistors. Four transistors are combined using T-junctions, and two four-transistor power cells are combined using a Wilkinson power combiner. Inter-stage matching networks use quarter-wave transformers separated by a series capacitor Y-inverter. The GaN MMIC has a chip size of  $3.3 \times 1.94\ \text{mm}^2$  and achieves a measured small-signal gain of 20 dB from 105 to 115 GHz. The measured output power at P5dB is around 28 to 29 dBm from 102 to 118 GHz with a PAE of 8%. The lower power PA achieves a measured power at 6 dB back-off of more than 25 dBm from 98 to 122 GHz. Furthermore, four GaN MMIC PAs of around 29 dBm output power were also used in a hybrid assembly with H-tee waveguide combiner (Fig. 39). The size of the solid-state power amplifier (SSPA) is  $5.4 \times 4.4 \times 1.9\ \text{cm}^3$ . The GaN SSPA achieves a measured output power of 34.4 dBm at 114 GHz and greater than 33 dBm from 102 to 116 GHz. The associated measured gain is 23 dB, and efficiency is around 6%. The measurements were done with waveguide fixtures and included losses of the integrated waveguide to microstrip transitions. Fig. 39 presents the SSPA module.

Likewise, a number of papers have been reported on InP PAs from 110 to 260 GHz. The dominant technology in this frequency regime is the InP HBT although a few advanced InP HEMT processes are also being used [184]. Some of the InP HBT processes that have been used for developing power amplifiers up to 260 GHz [11] are also summarised in Table I. The highest  $f_{\text{MAX}}$  of the 128 nm InP HBT is 1.3 THz with a 3.3 V breakdown voltage, and a current density of 2.3 mA/ $\mu\text{m}$  emitter length.

Single chip power amplifiers from 17 dBm to 23 dBm up to 260 GHz have been widely reported in these processes [40], [184]–[186]. In particular, a sub-50 nm InP HEMT process is used in a 207–230 GHz MMIC that delivers a 17 dBm output power with 11.5 dB small signal gain and an associated 2.3% PAE [185]. On the other hand, a 22.5 dBm MMIC with 22 dB small signal gain has also been demonstrated in [182] using a 250 nm InP HBT process. Due to low current density and low voltage operation, InP MMIC amplifiers employ as many as 16 parallel HBTs in the output stage. Specifically, authors in [40] have demonstrated a 17–24 dBm output power PA from 180–265 GHz in a single InP chip. The PA has been designed in a 250 nm HBT process. The common-emitter and common base HBT's are used to form a cascode cell with a total emitter periphery of 4-fingers  $\times$  6  $\mu\text{m}$  ( $L_e = 24\ \mu\text{m}$ ) for each device. The 3-stage amplifier is shown in Fig. 40 in which the last stage has a total of 16 parallel transistor cells. The 2:1 and 4:1 on-chip power combiners are used in the last stage, having insertion losses of 0.5 dB and 0.55 dB, respectively. The amplifier has a measured gain of 30 dB at 220 GHz and maintains more than 20 dB of gain from 190 to 260 GHz. The collector voltage operation is from 1.65 V to 2.2 V. The amplifier achieves a maximum output power of 23.4 dBm and higher than 20 dBm from 185 to 255 GHz.

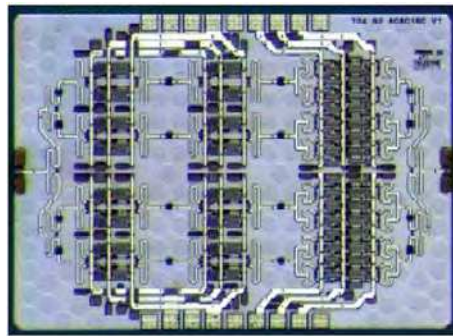


Fig. 40. 3-stage 16-way combined PA ( $2.14 \times 1.58\ \text{mm}^2$ ) [40] ©IEEE 2017.

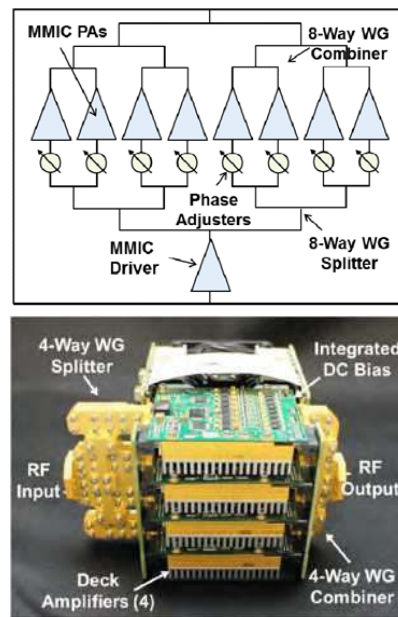


Fig. 41. G-Band amplifier formed by combining four deck amplifiers: block diagram of 8-way waveguide combiner deck amplifier (top), and 32-MMIC PA (bottom) [193] ©IEEE 2015.

The measured PAE is between 1.3% to 4.1% within the same band. Using the same 250 nm InP HBT process, the latest D-band MMIC demonstrates a measured gain of 29.5 dB with an outstanding PAE of 10.5% at 140 GHz [186]. However, the output power is still limited to 150 mW.

The InP MMICs have also been used to implement a multi-deck PA. In particular, Fig. 41(a) shows a 8-way waveguide combiner employed in a module that combines 8 InP MMICs to form one amplifier deck [193]. A phase shift is incorporated at each input of the single MMIC to adjust the phase for maximizing the combining efficiency. Four amplifier decks are then combined using a 4:1 WR-4 waveguide combiner/divider. The four-deck power amplifier module (32 MMICs) shown in Fig. 41(b) achieved 28.5 dBm saturated power at 230 GHz, and more than 32 dB small signal gain from 200 to 260 GHz. Amplifiers using InP HEMTs with 25 nm gate length have also been demonstrated to have 9 B of gain at 1 THz [194].

Besides InP, GaAs mHEMT is another technology that can provide very high frequency operation. GaAs mHEMT power

TABLE VII  
SOA PAS ABOVE 110 GHz.

Ref.	Year	Technology	Freq. (GHz)	Topology	N. of stages	$P_{SAT}$ (dBm)	PAE <sub>SAT</sub> (%)	SS Gain (dB)
[181]	2018	150 nm GaN HEMT	102–118	8-way combined	5	29.5	13	20
[183]	2018	100 nm GaN HEMT	115	cascode	4	20.3	2.6	34.8
[40]	2017	250 nm InP HBT	200–255	16-way combined	3	17–24	4.1	24
[187]	2015	35 nm GaAs mHEMT	250	4-way combined	3	10	2.9	32.8
[188]	2018	35 nm GaAs mHEMT	240	3-stacked	2	10.8	5	21.5
[189]	2017	130 nm SiGe BiCMOS	160	differential	5	15.5	7.2	30
[190]	2012	65 nm CMOS	140	8-way combined	4	13.2	14.6	16
[191]	2018	40 nm CMOS	140	2-way combined	3	14.8	8.9	20.3
[192]	2018	65 nm CMOS	114–131	differential	4	14.5	10.2	22.3

amplifiers have been demonstrated up to 330 GHz. Amplifiers using a 100 nm mHEMT process and a 50 nm mHEMT process have been demonstrated at 186–212 GHz [195] and 210–235 GHz [196], respectively. Both MMICs exhibits 7.5 dBm output power with around 2.5% PAE. Operating at frequencies higher than 200 GHz, the 35 nm mHEMT is the most up to date technology node of which the  $f_T$  and  $f_{MAX}$  are 515 GHz and 1000 GHz, respectively. The breakdown voltage of the process is around 2 V with a power density of 0.6 W/mm. Therefore, the GaAs mHEMT process is more suitable for developing low noise amplifiers at high frequency. The authors in [187] present a 32.8 dB gain PA at 250 GHz using the 35 nm mHEMT GaAs process. To improve the power, triple stacked-FET technique are used [36], [188]. The 240 GHz MMICs has a measured power of 10.8 dBm with 21.5 dB of gain, and the 300 GHz MMICs achieves 4.5 dBm output power with 11.6 dB of gain. Recently, a 238–292 GHz amplifier has also been presented with 6.7 dBm power with an associated maximum gain of 14.7 dB [197].

Silicon-based technologies have also been developed and deployed in mm-wave frequencies above 110 GHz. While SiGe and Si-CMOS have higher level of integration, their power amplifiers yield much lower power as compared to GaN MMICs. The 130 nm SiGe BiCMOS process is popular and has been used for developing power amplifiers to 255 GHz. For the 130 nm SiGe process, its  $f_T$  and  $f_{MAX}$  are 295 GHz and 400 GHz, respectively. The breakdown voltages BVCEO and BVCBO are 1.55 V and 6.0 V. A 170 GHz amplifier using the 130 nm SiGe process has been presented with up to 32 dB gain and 10 dBm output power [198]. To achieve high power, 4-way and 8-way on-chip power combiners are usually used in SiGe PAs. The typical output power is in the range of 7 to 15.5 dBm at different frequency ranging from 110 to 255 GHz [42], [189], [199], [200]. The highest output power achieved by SiGe amplifiers is 22 dBm at around 120 GHz [201]. The MMIC shown in Fig. 42 is fabricated in an advanced 90 nm SiGe BiCMOS process and demonstrates up to 22 dBm power with 7.7 dB gain and 3.6% PAE.

Si CMOS amplifiers have been demonstrated from 110 to 170 GHz. The output power is the lowest among all technologies and is in the range of 5 to 15 dBm. The most popular technology node in this frequency regime is 65 nm [137]. The authors in [190] presented a high efficiency D-band PA using 8-way power combiner in a 65 nm CMOS process. The 4-stage

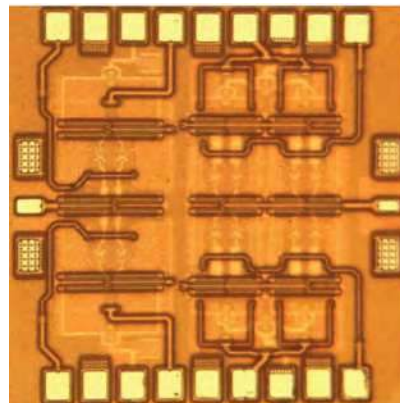


Fig. 42. 22 dBm 120 GHz MMIC using 90 nm InP SiGe BiCMOS process [201] ©IEEE 2018.

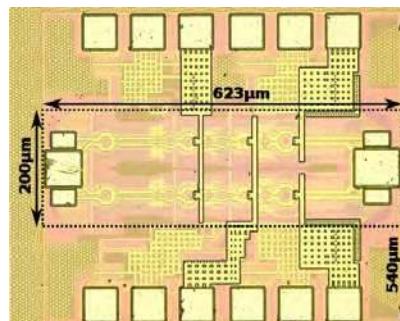


Fig. 43. 14.8 dBm PA in 40 nm CMOS employing 2-way transformer-based power combining [191] ©IEEE 2018.

circuit exhibits a measured output power of 13.2 dBm with an associated peak PAE of 14.6% at 140 GHz, which is among the highest efficiency achieved in the similar frequency range. Up to 22.3 dB gain and 14.5 dBm output power has been presented in a 114–131 GHz amplifier using the same 65 nm process [192]. Other CMOS processes such as FD SOI 28 nm and 40 nm CMOS have also been deployed in D-band PAs [191], [202]. The highest output power CMOS PA reported to date (shown in Fig. 43) was implemented in the 40 nm process. The design employing 2-way transformer-based power combining technique demonstrates a maximum power of 14.8 dBm with very high gain of 20.3 dB and peak PAE of 8.9% [191].

The state of the art in terms of output power, efficiency and bandwidth for the various technologies previously mentioned is reported in Table VII.

### VIII. CONCLUSION

This paper has provided an overview of the current state-of-the-art in power amplifiers in the whole millimeter-wave frequency range. The relevance of this topic is increasing steadily thanks to the drive from large scale applications such as 5G and satellite communications, providing a fertile environment for the exploration of new technology solutions and design techniques, as well as the adaptation of methods successfully adopted at lower frequency by the microwave community.

### REFERENCES

- [1] "IEEE Standard Letter Designations for Radar-Frequency Bands," *IEEE Std 521-2002 (Revision of IEEE Std 521-1984)*, pp. 1–10, Jan 2003.
- [2] H. Wang, F. Wang, S. Li, T.-Y. Huang, A. S. Ahmed, N. S. Mannem, J. Lee, E. Garay, D. Munzer, C. Snyder, S. Lee, H. T. Nguyen, and M. E. D. Smith, "Power amplifiers performance survey 2000-present," July 2019. [Online]. Available: [https://gems.ece.gatech.edu/PA\\_survey.html](https://gems.ece.gatech.edu/PA_survey.html)
- [3] B. Peterson and D. Schnauffer. (2018, Feb.) 5G Fixed Wireless Access Array and RF Front-End Trade-Offs. *Microwave Journal*. [Online]. Available: <https://www.microwavejournal.com/articles/29707-g-fixed-wireless-access-array-and-rf-front-end-trade-offs>
- [4] D. Danzilio. (2018, May) Advanced GaAs Integration for Single Chip mmWave Front-Ends. *Microwave Journal*. [Online]. Available: <https://www.microwavejournal.com/articles/30273-advanced-gaas-integration-for-single-chip-mmwave-front-ends>
- [5] UMS, "UMS Foundry Brochure 2019–2020," 2019. [Online]. Available: [https://www.ums-gaas.com/wp-content/uploads/2019/10/2019-2020\\_Brochure\\_Foundry\\_Low-version.pdf](https://www.ums-gaas.com/wp-content/uploads/2019/10/2019-2020_Brochure_Foundry_Low-version.pdf)
- [6] Z. Griffith, M. Urteaga, P. Rowell, and R. Pierson, "71–95 GHz (23–40% PAE) and 96–120 GHz (19–22% PAE) high efficiency 100–130 mW power amplifiers in InP HBT," in *2016 IEEE MTT-S International Microwave Symposium (IMS)*, May 2016, pp. 1–4.
- [7] OMMIC, "OMMIC Catalog 2019 v2," 2019. [Online]. Available: [https://www.ommic.com/wp-content/uploads/2019/09/OMMIC\\_Catalog-2019\\_V2.pdf](https://www.ommic.com/wp-content/uploads/2019/09/OMMIC_Catalog-2019_V2.pdf)
- [8] T. Shivan, M. Hossain, D. Stoppel, N. Weimann, S. Schulz, R. Doerner, V. Krozer, and W. Heinrich, "An Ultra-Broadband Low-Noise Distributed Amplifier in InP DHBT Technology," in *2018 13th European Microwave Integrated Circuits Conference (EuMIC)*, Sep. 2018, pp. 241–244.
- [9] D. P. Nguyen, A. N. Stameroff, and A. Pham, "A 1.5–88 GHz 19.5 dBm output power triple stacked HBT InP distributed amplifier," in *2017 IEEE MTT-S International Microwave Symposium (IMS)*, June 2017, pp. 20–23.
- [10] H. Hamada, T. Tsutsumi, G. Itami, H. Sugiyama, H. Matsuzaki, K. Okada, and H. Nosaka, "300-GHz 120-Gb/s Wireless Transceiver with High-Output-Power and High-Gain Power Amplifier Based on 80-nm InP-HEMT Technology," in *2019 IEEE BiCMOS and Compound Semiconductor Integrated Circuits and Technology Symposium (BCICTS)*, Nov 2019, pp. 1–4.
- [11] M. J. W. Rodwell, M. Le, and B. Brar, "InP Bipolar ICs: Scaling Roadmaps, Frequency Limits, Manufacturable Technologies," *Proc. IEEE*, vol. 96, no. 2, pp. 271–286, Feb 2008.
- [12] J. B. Hacker, W. Ha, C. Hillman, M. Urteaga, R. Pierson, and B. Brar, "Compact InP HBT Power Amplifiers Using Integrated Thick BCB Dielectrics," in *2007 IEEE/MTT-S International Microwave Symposium*, June 2007, pp. 805–808.
- [13] H. Hamada, T. Tsutsumi, H. Sugiyama, and H. Nosaka, "High-Output-Power and Reverse-Isolation G-Band Power Amplifier Module Based on 80-NM InP HEMT Technology," in *2018 Asia-Pacific Microwave Conference (APMC)*, Nov. 2018, pp. 633–635.
- [14] M. Yu, M. Matlobian, P. Petre, L. R. Hamilton, R. Bowen, M. Lui, H. Sun, C. M. Ngo, P. Janke, D. W. Baker, and R. S. Robertson, "W-band InP HEMT MMICs using finite-ground coplanar waveguide (FGCPW) design," *IEEE J. Solid-State Circuits*, vol. 34, no. 9, pp. 1212–1218, Sep. 1999.
- [15] B. Welp, K. Noujeim, and N. Pohl, "A Wideband 20 to 28 GHz Signal Generator MMIC With 30.8 dBm Output Power Based on a Power Amplifier Cell With 31% PAE in SiGe," *IEEE Journal of Solid-State Circuits*, vol. 51, no. 9, pp. 1975–1984, Sep. 2016.
- [16] J. Kim and J. F. Buckwalter, "A 1.1 THz Gain-Bandwidth W-Band Amplifier in a 0.12  $\mu\text{m}$  Silicon Germanium BiCMOS Process," *IEEE Microw. Wireless Compon. Lett.*, vol. 20, no. 11, pp. 625–627, Nov 2010.
- [17] M. Chang and G. M. Rebeiz, "A 26 to 40 GHz Wideband SiGe Balanced Power Amplifier IC," in *2007 IEEE Radio Frequency Integrated Circuits (RFIC) Symposium*, June 2007, pp. 729–732.
- [18] S. Li, D. Fritsche, C. Carta, and F. Ellinger, "Design and characterization of a 12–40 GHz power amplifier in SiGe technology," in *2018 IEEE Topical Conference on RF/Microwave Power Amplifiers for Radio and Wireless Applications (PAWR)*, Jan 2018, pp. 23–25.
- [19] M. Özen, N. Rostomyan, K. Aufinger, and C. Fager, "Efficient Millimeter Wave Doherty PA Design Based on a Low-Loss Combiner Synthesis Technique," *IEEE Microw. Wireless Compon. Lett.*, vol. 27, no. 12, pp. 1143–1145, Dec 2017.
- [20] S. Hu, F. Wang, and H. Wang, "A 28-/37-/39-GHz Linear Doherty Power Amplifier in Silicon for 5G Applications," *IEEE J. Solid-State Circuits*, vol. 54, no. 6, pp. 1586–1599, June 2019.
- [21] F. Wang and H. Wang, "A 24–30 GHz Watt-Level Broadband Linear Doherty Power Amplifier with Multi-Primary Distributed-Active-Transformer Power-Combining Supporting 5G NR FR2 64QAM with >19 dBm Average Pout and >19% Average PAE," in *2020 IEEE International Solid-State Circuits Conference (accepted and to appear)*, 2020.
- [22] J. Moron, R. Leblanc, F. Lecourt, and P. Frijlink, "12 W, 30% PAE, 40 GHz power amplifier MMIC using a commercially available GaN/Si process," in *2018 IEEE/MTT-S International Microwave Symposium - IMS*, June 2018, pp. 1457–1460.
- [23] S. Din, M. Wojtowicz, and M. Siddiqui, "High power and high efficiency Ka band power amplifier," in *2015 IEEE MTT-S International Microwave Symposium*, May 2015, pp. 1–4.
- [24] C. F. Campbell, K. Tran, M. Kao, and S. Nayak, "A K-Band 5W Doherty Amplifier MMIC Utilizing 0.15  $\mu\text{m}$  GaN on SiC HEMT Technology," in *2012 IEEE Compound Semiconductor Integrated Circuit Symposium (CSICS)*, Oct 2012, pp. 1–4.
- [25] M. Micovic, A. Kurdoghlian, H. P. Moyer, P. Hashimoto, A. Schmitz, I. Milosavjevic, P. J. Willadsen, W. S. Wong, J. Duvall, M. Hu, M. J. Delaney, and D. H. Chow, "Ka-band MMIC power amplifier in GaN HFET technology," in *2004 IEEE MTT-S International Microwave Symposium Digest (IEEE Cat. No.04CH37535)*, vol. 3, June 2004, pp. 1653–1656 Vol.3.
- [26] P. Neininger, L. John, P. Brückner, C. Friesicke, R. Quay, and T. Zwick, "Design, Analysis and Evaluation of a Broadband High-Power Amplifier for Ka-Band Frequencies," in *2019 IEEE MTT-S International Microwave Symposium (IMS)*, June 2019, pp. 564–567.
- [27] A. Margomenos, A. Kurdoghlian, M. Micovic, K. Shinohara, D. F. Brown, A. L. Corrión, H. P. Moyer, S. Bernham, D. C. Regan, R. M. Grabar, C. McGuire, M. D. Wetzel, R. Bowen, P. S. Chen, H. Y. Tai, A. Schmitz, H. Fung, A. Fung, and D. H. Chow, "GaN Technology for E, W and G-Band Applications," in *2014 IEEE Compound Semiconductor Integrated Circuit Symposium (CSICS)*, Oct 2014, pp. 1–4.
- [28] S. Pornpromlikit, H. Dabag, B. Hanafi, J. Kim, L. E. Larson, J. F. Buckwalter, and P. M. Asbeck, "A Q-Band Amplifier Implemented with Stacked 45-nm CMOS FETs," in *2011 IEEE Compound Semiconductor Integrated Circuit Symposium (CSICS)*, Oct 2011, pp. 1–4.
- [29] J. Plouchart, N. Zamdmer, Jonghae Kim, R. Trzcinski, S. Narasimha, M. Khare, L. F. Wagner, S. L. Sweeney, and S. Chaloux, "A 243-GHz F/sub t/ and 208-GHz F/sub max/, 90-nm SOI CMOS SoC technology with low-power mm-wave digital and RF circuit capability," *IEEE Trans. Electron Devices*, vol. 52, no. 7, pp. 1370–1375, July 2005.
- [30] F. Wang, T. Li, and H. Wang, "A Highly Linear Super-Resolution Mixed-Signal Doherty Power Amplifier for High-Efficiency mm-Wave 5G Multi-Gb/s Communications," in *2019 IEEE International Solid-State Circuits Conference - (ISSCC)*, Feb 2019, pp. 88–90.
- [31] N. Rostomyan, M. Özen, and P. Asbeck, "28 GHz Doherty Power Amplifier in CMOS SOI With 28% Back-Off PAE," *IEEE Microw. Wireless Compon. Lett.*, vol. 28, no. 5, pp. 446–448, May 2018.



- [32] K. Shinohara, D. C. Regan, Y. Tang, A. L. Corrion, D. F. Brown, J. C. Wong, J. F. Robinson, H. H. Fung, A. Schmitz, T. C. Oh, S. J. Kim, P. S. Chen, R. G. Nagele, A. D. Margomenos, and M. Micovic, "Scaling of GaN HEMTs and Schottky Diodes for Submillimeter-Wave MMIC Applications," *IEEE Trans. Electron Devices*, vol. 60, no. 10, pp. 2982–2996, Oct. 2013.
- [33] A. Margomenos, A. Kurdoghlian, M. Micovic, K. Shinohara, D. F. Brown, A. L. Corrion, H. P. Moyer, S. Burnham, D. C. Regan, R. M. Grabar, C. McGuire, M. D. Wetzel, R. Bowen, P. S. Chen, H. Y. Tai, A. Schmitz, H. Fung, A. Fung, and D. H. Chow, "GaN Technology for E, W and G-Band Applications," in *2014 IEEE Compound Semiconductor Integrated Circuit Symposium (CSICS)*, Oct. 2014, pp. 1–4.
- [34] H. Chandrasekar, M. J. Uren, M. A. Casbon, H. Hirshy, A. Eblabla, K. Elgaid, J. W. Pomeroy, P. J. Tasker, and M. Kuball, "Quantifying Temperature-Dependent Substrate Loss in GaN-on-Si RF Technology," *IEEE Trans. Electron Devices*, vol. 66, no. 4, pp. 1681–1687, April 2019.
- [35] S. Diebold, P. Pahl, B. Goettel, H. Massler, A. Tessmann, A. Leuther, T. Zwick, and I. Kallfass, "A 130 to 160 GHz broadband power amplifier with binary power splitting topology," in *2012 Asia Pacific Microwave Conference Proceedings*, Dec 2012, pp. 442–444.
- [36] A. B. Amado-Rey, Y. Campos-Roca, C. Friesicke, S. Wagner, and O. Ambacher, "GCPW GaAs Broadside Couplers at H-Band and Application to Balanced Power Amplifiers," *IEEE Trans. Microw. Theory Techn.*, vol. 67, no. 1, pp. 78–85, Jan 2019.
- [37] H. Kazemi, D. Miller, A. Mohan, Z. Griffith, Y. Jin, J. Kwiatkowski, L. Tran, and M. Crawford, "350mW G-band medium power amplifier fabricated through a new method of 3D-copper additive manufacturing," in *2015 IEEE MTT-S International Microwave Symposium*, May 2015, pp. 1–3.
- [38] D. Gritters, K. Brown, and E. Ko, "200–260GHz solid state amplifier with 700mW of output power," in *2015 IEEE MTT-S International Microwave Symposium*, May 2015, pp. 1–3.
- [39] T. B. Reed, Z. Griffith, P. Rowell, M. Field, and M. Rodwell, "A 180mW InP HBT Power Amplifier MMIC at 214 GHz," in *2013 IEEE Compound Semiconductor Integrated Circuit Symposium (CSICS)*, Oct. 2013, pp. 1–4.
- [40] Z. Griffith, M. Urteaga, and P. Rowell, "180–265 GHz, 17–24 dBm output power broadband, high-gain power amplifiers in InP HBT," in *2017 IEEE MTT-S International Microwave Symposium (IMS)*, June 2017, pp. 973–976.
- [41] Z. Griffith, M. Urteaga, P. Rowell, and R. Pierson, "190–260 GHz High-Power, Broadband PA's in 250 nm InP HBT," in *2015 IEEE Compound Semiconductor Integrated Circuit Symposium (CSICS)*, Oct. 2015, pp. 1–4.
- [42] M. H. Eissa and D. Kissinger, "A 13.5dBm Fully Integrated 200-to-255GHz Power Amplifier with a 4-Way Power Combiner in SiGe:C BiCMOS," in *2019 IEEE International Solid-State Circuits Conference - (ISSCC)*, Feb 2019, pp. 82–84.
- [43] Z. Wang, P. Chiang, P. Nazari, C. Wang, Z. Chen, and P. Heydari, "A CMOS 210-GHz Fundamental Transceiver With OOK Modulation," *IEEE J. Solid-State Circuits*, vol. 49, no. 3, pp. 564–580, Mar. 2014.
- [44] Y. Zhang and P. Reynaert, "A high-efficiency linear power amplifier for 28GHz mobile communications in 40nm CMOS," in *2017 IEEE Radio Frequency Integrated Circuits Symposium (RFIC)*, June 2017, pp. 33–36.
- [45] J. Lee and S. Heo, "A 27 GHz, 14 dBm CMOS Power Amplifier Using 0.18  $\mu\text{m}$  Common-Source MOSFETs," *IEEE Microw. Wireless Compon. Lett.*, vol. 18, no. 11, pp. 755–757, Nov. 2008.
- [46] J. Essing, D. Leenaerts, and R. Mahmoudi, "A 27GHz, 31dBm power amplifier in a 0.25  $\mu\text{m}$  SiGe:C BiCMOS technology," in *2014 IEEE Bipolar/BiCMOS Circuits and Technology Meeting (BCTM)*, Sep. 2014, pp. 143–146.
- [47] J. J. Pekarik, J. Adkisson, P. Gray, Q. Liu, R. Camillo-Castillo, M. Khater, V. Jain, B. Zetterlund, A. DiVergilio, X. Tian, A. Vallett, J. Ellis-Monaghan, B. J. Gross, P. Cheng, V. Kaushal, Z. He, J. Lukaitis, K. Newton, M. Kerbaugh, N. Cahoon, L. Vera, Y. Zhao, J. R. Long, A. Valdes-Garcia, S. Reynolds, W. Lee, B. Sadhu, and D. Hareme, "A 90 nm SiGe BiCMOS technology for mm-wave and high-performance analog applications," in *2014 IEEE Bipolar/BiCMOS Circuits and Technology Meeting (BCTM)*, Sep. 2014, pp. 92–95.
- [48] C. J. Zhang, J. Ma, G. Y. Li, Y. Kishiyama, S. Parkvall, G. Liu, and Y. Kim, "Key Technology for 5G New Radio," *IEEE Commun. Mag.*, vol. 56, no. 3, pp. 10–11, Mar. 2018.
- [49] Y. Cho, W. Lee, H. Park, B. Park, J. H. Lee, J. Kim, J. Lee, S. Kim, J. Park, S. Park, K. H. An, J. Son, and S. Yang, "A 16-Element Phased-Array CMOS Transmitter with Variable Gain Controlled Linear Power Amplifier for 5G New Radio," in *2019 IEEE Radio Frequency Integrated Circuits Symposium (RFIC)*, June 2019, pp. 247–250.
- [50] W. Roh, J. Seol, J. Park, B. Lee, J. Lee, Y. Kim, J. Cho, K. Cheun, and F. Aryanfar, "Millimeter-wave beamforming as an enabling technology for 5G cellular communications: theoretical feasibility and prototype results," *IEEE Commun. Mag.*, vol. 52, no. 2, pp. 106–113, Feb. 2014.
- [51] S. Cripps, *RF power amplifiers for wireless communications*, ser. Artech House Microwave Library. Artech House, 2006.
- [52] P. Colantonio, F. Giannini, and E. Limiti, *High Efficiency RF and Microwave Solid State Power Amplifiers*, ser. Microwave and Optical Engineering. John Wiley & Sons, 2009.
- [53] H. Wang, C. Sideris, and A. Hajimiri, "A CMOS Broadband Power Amplifier With a Transformer-Based High-Order Output Matching Network," *IEEE Journal of Solid-State Circuits*, vol. 45, no. 12, pp. 2709–2722, Dec 2010.
- [54] S. Cripps, P. Tasker, A. Clarke, J. Lees, and J. Benedikt, "On the Continuity of High Efficiency Modes in Linear RF Power Amplifiers," *IEEE Microw. Wireless Compon. Lett.*, vol. 19, no. 10, pp. 665 – 667, Oct. 2009.
- [55] V. Carrubba, A. L. Clarke, M. Akmal, J. Lees, J. Benedikt, P. J. Tasker, and S. C. Cripps, "On the extension of the continuous Class-F mode power amplifier," *IEEE Trans. Microw. Theory Techn.*, vol. 59, no. 5, pp. 1294–1303, May 2011.
- [56] J. R. Powell, M. J. Uren, T. Martin, A. McLachlan, P. Tasker, S. Woodington, J. Bell, R. Saini, J. Benedikt, and S. C. Cripps, "GaAs X-band high efficiency (>65%) Broadband (>30%) amplifier MMIC based on the Class B to Class J continuum," in *2011 IEEE MTT-S International Microwave Symposium*, June 2011, pp. 1–4.
- [57] T. Li, M. Huang, and H. Wang, "A continuous-mode harmonically tuned 19-to-29.5GHz ultra-linear PA supporting 18Gb/s at 18.4% modulation PAE and 43.5% peak PAE," in *2018 IEEE International Solid - State Circuits Conference - (ISSCC)*, Feb 2018, pp. 410–412.
- [58] —, "Millimeter-Wave Continuous-Mode Power Amplifier for 5G MIMO Applications," *IEEE Transactions on Microwave Theory and Techniques*, vol. 67, no. 7, pp. 3088–3098, July 2019.
- [59] R. Quaglia, J. J. Bell, and S. Cripps, "New general formulation and experimental verification of harmonic clipping contours in high-frequency power devices," *IEEE Trans. Microw. Theory Techn.*, vol. 65, no. 10, pp. 3903–3909, Oct. 2017.
- [60] M. Micovic, A. Kurdoghlian, H. P. Moyer, P. Hashimoto, M. Hu, M. Antcliffe, P. J. Willadsen, W. S. Wong, R. Bowen, I. Milosavljevic, Y. Yoon, A. Schmitz, M. Wetzel, C. McGuire, B. Hughes, and D. H. Chow, "GaN MMIC PAs for E-Band (71 GHz – 95 GHz) Radio," in *2008 IEEE Compound Semiconductor Integrated Circuits Symposium*, Oct 2008, pp. 1–4.
- [61] N. Sarmah, K. Aufinger, R. Lachner, and U. R. Pfeiffer, "A 200–225 GHz SiGe Power Amplifier with peak Psat of 9.6 dBm using wideband power combination," in *ESSIRC Conference 2016: 42nd European Solid-State Circuits Conference*, Sep. 2016, pp. 193–196.
- [62] Kim-Lien Ngo-Wah, J. Goel, Yeong-Chang Chou, R. Grundbacher, R. Lai, G. Nassour, E. Divish, G. Schreyer, K. Whitney, and A. Oki, "A V-band eight-way combined solid-state power amplifier with 12.8 Watt output power," in *IEEE MTT-S International Microwave Symposium Digest, 2005.*, June 2005, pp. 4 pp.–.
- [63] Huei Wang, R. Lai, M. Biedenbender, G. S. Dow, and B. R. Allen, "Novel W-band monolithic push-pull power amplifiers," *IEEE J. Solid-State Circuits*, vol. 30, no. 10, pp. 1055–1061, Oct. 1995.
- [64] J. M. Schellenberg, "A broadband, push-pull power MMIC operating at K/Ka-band frequencies," in *2002 IEEE MTT-S International Microwave Symposium Digest*, vol. 2, June 2002, pp. 909–912 vol.2.
- [65] S. Kulkarni and P. Reynaert, "A Push-Pull mm-Wave power amplifier with <math><0.8^\circ</math> AM-PM distortion in 40 nm CMOS," in *2014 IEEE International Solid-State Circuits Conference*, Feb 2014, pp. 252–253.
- [66] T. Li and H. Wang, "A Continuous-Mode 23.5–41 GHz Hybrid Class-F/F-1 Power Amplifier with 46% Peak PAE for 5G Massive MIMO Applications," in *2018 IEEE Radio Frequency Integrated Circuits Symposium (RFIC)*, June 2018, pp. 220–230.
- [67] M. Thian, M. Tiebout, N. B. Buchanan, V. F. Fusco, and F. Dielacher, "A 76–84 GHz SiGe power amplifier array employing low-loss four-way differential combining transformer," *IEEE Trans. Microw. Theory Techn.*, vol. 61, no. 2, pp. 931–938, Feb. 2013.
- [68] E. Kaymaksut, D. Zhao, and P. Reynaert, "Transformer-Based Doherty Power Amplifiers for mm-Wave Applications in 40-nm CMOS," *IEEE Trans. Microw. Theory Techn.*, vol. 63, no. 4, pp. 1186–1192, April 2015.
- [69] D. Chowdhury, P. Reynaert, and A. M. Niknejad, "Design Considerations for 60 GHz Transformer-Coupled CMOS Power Amplifiers,"

- IEEE Journal of Solid-State Circuits*, vol. 44, no. 10, pp. 2733–2744, Oct 2009.
- [70] H. Park, S. Daneshgar, J. C. Rode, Z. Griffith, M. Urteaga, B. Kim, and M. Rodwell, “30% PAE W-Band InP power amplifiers using sub-quarter-wavelength baluns for series-connected power-combining,” in *2013 IEEE Compound Semiconductor Integrated Circuit Symposium (CSICS)*, Oct 2013, pp. 1–4.
- [71] H. Dabag, B. Hanafi, F. Golcuk, A. Agah, J. F. Buckwalter, and P. M. Asbeck, “Analysis and Design of Stacked-FET Millimeter-Wave Power Amplifiers,” *IEEE Trans. Microw. Theory Techn.*, vol. 61, no. 4, pp. 1543–1556, April 2013.
- [72] M. Gavell, I. Angelov, M. Ferndahl, and H. Zirath, “A high voltage mm-wave stacked HEMT power amplifier in 0.1  $\mu\text{m}$  InGaAs technology,” in *2015 IEEE MTT-S International Microwave Symposium*, May 2015, pp. 1–3.
- [73] A. B. Amado-Rey, Y. Campos-Roca, F. van Raay, C. Friesicke, S. Wagner, H. Massler, A. Leuther, and O. Ambacher, “Analysis and Development of Submillimeter-Wave Stacked-FET Power Amplifier MMICs in 35-nm mHEMT Technology,” *IEEE Trans. on Terahertz Science and Techn.*, vol. 8, no. 3, pp. 357–364, May 2018.
- [74] C. F. Campbell, S. Nayak, Ming-Yih Kao, and Shuoqi Chen, “Design and performance of 16–40GHz GaN distributed power amplifier MMICs utilizing an advanced 0.15  $\mu\text{m}$  GaN process,” in *2016 IEEE MTT-S International Microwave Symposium (IMS)*, May 2016, pp. 1–4.
- [75] M. J. Schindler, J. P. Wendler, M. P. Zaitlin, M. E. Miller, and J. R. Dormail, “A K/Ka-band distributed power amplifier with capacitive drain coupling,” *IEEE Trans. Microw. Theory Techn.*, vol. 36, no. 12, pp. 1902–1907, Dec. 1988.
- [76] T. Shivan, M. Hossain, R. Doerner, S. Schulz, T. Johansen, S. Boppel, W. Heinrich, and V. Krozer, “A 175 GHz Bandwidth High Linearity Distributed Amplifier in 500 nm InP DHBT Technology,” in *2019 IEEE MTT-S International Microwave Symposium (IMS)*, June 2019, pp. 1253–1256.
- [77] S. Yoon, I. Lee, M. Urteaga, M. Kim, and S. Jeon, “A Fully-Integrated 40–222 GHz InP HBT Distributed Amplifier,” *IEEE Microw. Wireless Compon. Lett.*, vol. 24, no. 7, pp. 460–462, July 2014.
- [78] T. Jyo, M. Nagatani, M. Ida, M. Mutoh, H. Wakita, N. Terao, and H. Nosaka, “A 241-GHz-Bandwidth Distributed Amplifier with 10-dBm P1dB in 0.25- $\mu\text{m}$  InP DHBT Technology,” in *2019 IEEE MTT-S International Microwave Symposium (IMS)*, June 2019, pp. 1430–1433.
- [79] Jonghae Kim, J. Plouchart, N. Zamdmer, R. Trzcenski, R. Groves, M. Sherony, Y. Tan, M. Talbi, J. Safran, and L. Wagner, “A 12dBm 320GHz GBW distributed amplifier in a 0.12  $\mu\text{m}$  SOI CMOS,” in *2004 IEEE International Solid-State Circuits Conference*, Feb. 2004, pp. 478–540 Vol.1.
- [80] J. Chen and A. M. Niknejad, “Design and analysis of a stage-scaled distributed power amplifier,” *IEEE Trans. Microw. Theory Techn.*, vol. 59, no. 5, pp. 1274–1283, May 2011.
- [81] K. Kim and C. Nguyen, “A Concurrent Ku/K/Ka Tri-Band Distributed Power Amplifier With Negative-Resistance Active Notch Using SiGe BiCMOS Process,” *IEEE Trans. Microw. Theory Techn.*, vol. 62, no. 1, pp. 125–136, Jan. 2014.
- [82] K. Fang, C. Levy, and J. F. Buckwalter, “A 105-GHz, supply-scaled distributed amplifier in 90-nm SiGe BiCMOS,” in *2015 IEEE Bipolar/BiCMOS Circuits and Technology Meeting*, Oct. 2015, pp. 182–185.
- [83] P. Dennler, D. Schwantuschke, R. Quay, and O. Ambacher, “8–42 GHz GaN non-uniform distributed power amplifier MMICs in microstrip technology,” in *2012 IEEE/MTT-S International Microwave Symposium Digest*, June 2012, pp. 1–3.
- [84] C. F. Campbell, “GaN non-uniform distributed power amplifier MMICs – The highs and lows (Invited),” in *2017 IEEE Compound Semiconductor Integrated Circuit Symposium (CSICS)*, Oct 2017, pp. 1–4.
- [85] N. Kalantari and J. F. Buckwalter, “A 91 to 110-GHz tapered constructive wave power amplifier in a 0.12  $\mu\text{m}$  SiGe BiCMOS process,” in *2010 IEEE Bipolar/BiCMOS Circuits and Technology Meeting (BCTM)*, Oct. 2010, pp. 125–128.
- [86] *3GPP 5G Mobile Broadband Standard Release 15*, 3GPP Std. release 15, 2017.
- [87] M. Agiwal, A. Roy, and N. Saxena, “Next Generation 5G Wireless Networks: A Comprehensive Survey,” *IEEE Communications Surveys Tutorials*, vol. 18, no. 3, pp. 1617–1655, thirdquarter 2016.
- [88] V. Camarchia, M. Pirola, and R. Quaglia, *Electronics for Microwave Backhaul*, ser. Artech House microwave library. Artech House Publishers, 2016. [Online]. Available: <https://books.google.it/books?id=RG6uDgAAQBAJ>
- [89] J. Christensen, *ITU Regulations for Ka-band Satellite Networks*, pp. 524–527. [Online]. Available: <https://arc.aiaa.org/doi/abs/10.2514/6.2012-15179>
- [90] B. Kim, H. Q. Tserng, and H. D. Shih, “44-GHz monolithic GaAs FET amplifier,” *IEEE Electron Device Lett.*, vol. 7, no. 2, pp. 95–97, Feb 1986.
- [91] J. Berenz, M. LaCon, and M. Luong, “Single chip Ka-band transceiver,” in *1991 IEEE MTT-S International Microwave Symposium Digest*, July 1991, pp. 517–520 vol.2.
- [92] D. L. Ingram, D. I. Stones, J. H. Elliott, Huei Wang, R. Lai, and M. Biedenbender, “A 6-W Ka-band power module using MMIC power amplifiers,” *IEEE Trans. Microw. Theory Techn.*, vol. 45, no. 12, pp. 2424–2430, Dec 1997.
- [93] M. K. Siddiqui, A. K. Sharma, L. G. Callejo, and R. Lai, “A high-power and high-efficiency monolithic power amplifier at 28 GHz for LMDS applications,” *IEEE Trans. Microw. Theory Techn.*, vol. 46, no. 12, pp. 2226–2232, Dec 1998.
- [94] —, “A high power broadband monolithic power amplifier for ka-band ground terminals,” in *1999 IEEE MTT-S International Microwave Symposium Digest (Cat. No.99CH36282)*, vol. 3, June 1999, pp. 951–954 vol.3.
- [95] Sung-Gi Yang and Kwang-Seok Seo, “A compact and wideband GaAs P-HEMT distributed amplifier IC based on a micro-machined CPW,” in *2000 IEEE MTT-S International Microwave Symposium Digest*, vol. 1, June 2000, pp. 213–216 vol.1.
- [96] Y. Sasaki, H. Kurusu, H. Hoshi, T. Hisaka, and Y. Mitsui, “20-30 GHz broadband MMIC power amplifiers with compact flat gain PHEMT cells,” in *2001 IEEE MTT-S International Microwave Symposium Digest (Cat. No.01CH37157)*, vol. 2, May 2001, pp. 1067–1070 vol.2.
- [97] Y. C. Lee and C. S. Park, “17-36 GHz broadband PHEMT MMIC power amplifier for point-to-multipoint applications,” in *2001 6th International Conference on Solid-State and Integrated Circuit Technology. Proceedings (Cat. No.01EX443)*, vol. 2, Oct 2001, pp. 1320–1323 vol.2.
- [98] P. Huang, Z. Tsai, K. Lin, and H. Wang, “A 17–35 GHz Broadband, High Efficiency PHEMT Power Amplifier Using Synthesized Transformer Matching Technique,” *IEEE Trans. Microw. Theory Techn.*, vol. 60, no. 1, pp. 112–119, Jan 2012.
- [99] P. Dennler, R. Quay, P. Brückner, M. Schlechtweg, and O. Ambacher, “Watt-level non-uniform distributed 6–37 GHz power amplifier MMIC with dual-gate driver stage in GaN technology,” in *2014 IEEE Topical Conference on Power Amplifiers for Wireless and Radio Applications (PAWR)*, Jan 2014, pp. 37–39.
- [100] C. F. Campbell, Ming-Yih Kao, and S. Nayak, “High efficiency Ka-band power amplifier MMICs fabricated with a 0.15  $\mu\text{m}$  GaN on SiC HEMT process,” in *2012 IEEE/MTT-S International Microwave Symposium Digest*, June 2012, pp. 1–3.
- [101] M. Roberg, T. R. Mya Kywe, M. Irvine, O. Marrufo, and S. Nayak, “40W Ka-Band Single and Dual Output GaN MMIC Power Amplifiers on SiC,” in *2018 IEEE BiCMOS and Compound Semiconductor Integrated Circuits and Technology Symposium (BCICTS)*, Oct 2018, pp. 140–143.
- [102] H. Otsuka, K. Yamauchi, K. Yamanaka, S. Chaki, K. Nakahara, K. Endo, A. Inoue, and Y. Hirano, “A Q-band 6W MMIC power amplifier with 3-way power combination circuit,” in *2010 IEEE Radio Frequency Integrated Circuits Symposium*, May 2010, pp. 171–174.
- [103] S. M. Haque, D. J. Hoppe, and L. W. Epp, “Solid state power amplifier and travelling wave tube amplifier additive phase noise characterization at Ka-band operation,” in *2009 IEEE Radar Conference*, May 2009, pp. 1–4.
- [104] P. M. Smith, D. Dugas, K. Chu, K. Nichols, K. G. Duh, J. Fisher, L. Mt Pleasant, D. Xu, L. Gunter, A. Vera, R. Lender, and D. Meharry, “Progress in GaAs metamorphic HEMT technology for microwave applications,” in *25th Annual Technical Digest 2003. IEEE Gallium Arsenide Integrated Circuit (GaAs IC) Symposium, 2003.*, Nov 2003, pp. 21–24.
- [105] M. Varonen, M. Karkkainen, M. Kantanen, T. Karttaavi, P. Kangaslahti, and K. Halonen, “Millimetre wave metamorphic HEMT amplifiers,” in *Proceedings Norchip Conference, 2004.*, Nov 2004, pp. 8–11.
- [106] M. V. Aust, A. K. Sharma, and A. L. Gutierrez-Aitken, “A high power and high efficiency 20 GHz InP HBT monolithic power amplifier for phased array applications,” in *2008 IEEE MTT-S International Microwave Symposium Digest*, June 2008, pp. 1127–1130.
- [107] B. Park, S. Jin, D. Jeong, J. Kim, Y. Cho, K. Moon, and B. Kim, “Highly Linear mm-Wave CMOS Power Amplifier,” *IEEE Trans. Microw. Theory Techn.*, vol. 64, no. 12, pp. 4535–4544, Dec 2016.

- [108] W. Huang, J. Lin, Y. Lin, and H. Wang, "A K-Band Power Amplifier with 26-dBm Output Power and 34% PAE with Novel Inductance-based Neutralization in 90-nm CMOS," in *2018 IEEE Radio Frequency Integrated Circuits Symposium (RFIC)*, June 2018, pp. 228–231.
- [109] F. Wang and H. Wang, "An Instantaneously Broadband Ultra-Compact Highly Linear PA with Compensated Distributed Balun Output Network Achieving  $>17.8$  dBm  $P_{1dB}$  and  $>36.6\%$   $PAE_{P_{1dB}}$  over 24–40GHz and Continuously Supporting 64-/256-QAM 5G NR Signals over 24–42GHz," in *2020 IEEE International Solid-State Circuits Conference (accepted and to appear)*, 2020.
- [110] R. Bhat, A. Chakrabarti, and H. Krishnaswamy, "Large-Scale Power Combining and Mixed-Signal Linearizing Architectures for Watt-Class mmWave CMOS Power Amplifiers," *IEEE Trans. Microw. Theory Techn.*, vol. 63, no. 2, pp. 703–718, Feb 2015.
- [111] D. Jeong, K. Moon, S. Lee, B. Park, J. Kim, J. Son, and B. Kim, "Linear CMOS power amplifier at Ka-band with ultra-wide video bandwidth," in *2017 IEEE Radio Frequency Integrated Circuits Symposium (RFIC)*, June 2017, pp. 220–223.
- [112] W. Doherty, "A new high efficiency power amplifier for modulated waves," *Proc. IRE*, vol. 24, no. 9, pp. 1163 – 1182, Sep. 1936.
- [113] V. Camarchia, M. Pirola, R. Quaglia, S. Jee, Y. Cho, and B. Kim, "The Doherty power amplifier: Review of recent solutions and trends," *IEEE Trans. Microw. Theory Techn.*, vol. 63, no. 2, pp. 559–571, Feb. 2015.
- [114] C. F. Campbell, "A fully integrated Ku-band Doherty amplifier MMIC," *IEEE Microwave and Guided Wave Letters*, vol. 9, no. 3, pp. 114–116, March 1999.
- [115] C. P. McCarroll, G. D. Alley, S. Yates, and R. Matreci, "A 20 GHz Doherty power amplifier MMIC with high efficiency and low distortion designed for broad band digital communication systems," in *2000 IEEE MTT-S International Microwave Symposium Digest (Cat. No.00CH37017)*, vol. 1, June 2000, pp. 537–540 vol.1.
- [116] V. Camarchia, J. J. M. Rubio, M. Pirola, R. Quaglia, P. Colantonio, F. Giannini, R. Giofrè, L. Piazzon, T. Emanuelsson, and T. Wegeland, "High-Efficiency 7 GHz Doherty GaN MMIC Power Amplifiers for Microwave Backhaul Radio Links," *IEEE Transactions on Electron Devices*, vol. 60, no. 10, pp. 3592–3595, Oct 2013.
- [117] R. Quaglia, V. Camarchia, T. Jiang, M. Pirola, S. Donati Guerrieri, and B. Loran, "K-Band GaAs MMIC Doherty Power Amplifier for Microwave Radio With Optimized Driver," *IEEE Trans. Microw. Theory Techn.*, vol. 62, no. 11, pp. 2518–2525, Nov 2014.
- [118] R. Quaglia, V. Camarchia, J. J. Moreno Rubio, M. Pirola, and G. Ghione, "A 4-W Doherty Power Amplifier in GaN MMIC Technology for 15-GHz Applications," *IEEE Microw. Wireless Compon. Lett.*, vol. 27, no. 4, pp. 365–367, April 2017.
- [119] D. P. Nguyen, J. Curtis, and A. V. Pham, "A Doherty amplifier with modified load modulation scheme based on load-pull data," *IEEE Trans. Microw. Theory Techn.*, vol. PP, no. 99, pp. 1–10, 2017.
- [120] G. Lv, W. Chen, and Z. Feng, "A Compact and Broadband Ka-band Asymmetrical GaAs Doherty Power Amplifier MMIC for 5G Communications," in *2018 IEEE/MTT-S International Microwave Symposium - IMS*, June 2018, pp. 808–811.
- [121] D. P. Nguyen, T. Pham, and A. Pham, "A 28-GHz Symmetrical Doherty Power Amplifier Using Stacked-FET Cells," *IEEE Trans. Microw. Theory Techn.*, vol. 66, no. 6, pp. 2628–2637, June 2018.
- [122] D. P. Nguyen, B. L. Pham, and A. Pham, "A compact ka-band integrated doherty amplifier with reconfigurable input network," *IEEE Trans. Microw. Theory Techn.*, vol. 67, no. 1, pp. 205–215, Jan 2019.
- [123] R. Giofrè, A. Del Gaudio, and E. Limiti, "A 28 GHz MMIC Doherty Power Amplifier in GaN on Si Technology for 5G Applications," in *2019 IEEE MTT-S International Microwave Symposium (IMS)*, June 2019, pp. 611–613.
- [124] F. Lam, M. Matloubian, A. Igawa, C. Chou, A. Kurdoghlian, C. Ngo, L. Jelloian, A. Brown, M. Thompson, and L. Larson, "44-GHz high-efficiency InP-HEMT MMIC power amplifier," *IEEE Microwave and Guided Wave Letters*, vol. 4, no. 8, pp. 277–278, Aug 1994.
- [125] L. A. Belov, V. N. Kochemasov, and S. M. Smolskiy, *Handbook of RF, microwave, and millimeter-wave components*. Boston: Artech House, 2012. [Online]. Available: <http://ebookcentral.proquest.com/lib/utk/detail.action?docID=1075917>
- [126] T. S. Rappaport, Y. Xing, G. R. MacCartney, A. F. Molisch, E. Mellios, and J. Zhang, "Overview of Millimeter Wave Communications for Fifth-Generation (5G) Wireless Networks—With a Focus on Propagation Models," *IEEE Trans. Antennas Propag.*, vol. 65, no. 12, pp. 6213–6230, Dec 2017.
- [127] *IEEE 802.11ad Microwave Wi-Fi/WiGig Tutorial*, IEEE Std., 2019. [Online]. Available: <https://ieeexplore.ieee.org/document/6392842>
- [128] Y. Ghasempour, C. R. C. M. da Silva, C. Cordeiro, and E. W. Knightly, "IEEE 802.11ay: Next-Generation 60 GHz Communication for 100 Gb/s Wi-Fi," *IEEE Communications Magazine*, vol. 55, no. 12, pp. 186–192, Dec 2017.
- [129] M. V. Aust, A. K. Sharma, O. Fordham, R. Grundbacher, R. To, R. Tsai, and R. Lai, "A highly efficient Q-band MMIC 2.8 Watt output power amplifier based on 0.15 $\mu$ m InGaAs/GaAs pHEMT process technology," in *IEEE Compound Semiconductor Integrated Circuit Symposium, 2005. CSIC '05.*, Oct 2005, pp. 4 pp.–.
- [130] Kim-Lien Ngo-Wah, J. Goel, Yeong-Chang Chou, R. Grundbacher, R. Lai, G. Nassour, E. Divish, G. Schreyer, K. Whitney, and A. Oki, "A V-band eight-way combined solid-state power amplifier with 12.8 Watt output power," in *IEEE MTT-S International Microwave Symposium Digest, 2005.*, June 2005, pp. 4 pp.–.
- [131] A. Bessemoulin, J. Tarazi, M. Rodriguez, M. G. McCulloch, A. E. Parker, and S. J. Mahon, "Reduced-size E-band GaAs power amplifier MMIC," in *2015 10th European Microwave Integrated Circuits Conference (EuMIC)*, Sep. 2015, pp. 25–28.
- [132] D. Schwantuschke, B. Godejohann, P. Brückner, A. Tessmann, and R. Quay, "mm-Wave operation of AlN/GaN-devices and MMICs at V-W-band," in *2018 22nd International Microwave and Radar Conference (MIKON)*, May 2018, pp. 238–241.
- [133] S. M. J. Liu, O. S. A. Tang, W. Kong, K. Nichols, J. Heaton, and P. C. Chao, "High efficiency monolithic InP HEMT V-band power amplifier," in *GaAs IC Symposium. IEEE Gallium Arsenide Integrated Circuit Symposium. 21st Annual. Technical Digest 1999 (Cat. No.99CH36369)*, Oct 1999, pp. 145–147.
- [134] Z. Griffith, M. Urteaga, P. Rowell, and R. Pierson, "340-440 mW Broadband, High-Efficiency E-Band PA's in InP HBT," in *2015 IEEE Compound Semiconductor Integrated Circuit Symposium (CSICS)*, Oct 2015, pp. 1–4.
- [135] H. T. Nguyen, D. Jung, and H. Wang, "A 60 GHz CMOS Power Amplifier with Cascaded Asymmetric Distributed-Active-Transformer Achieving Watt-Level Peak Output Power with 20.8% PAE and Supporting 2Gsym/s 64-QAM Modulation," in *2019 IEEE International Solid-State Circuits Conference - (ISSCC)*, Feb 2019, pp. 90–92.
- [136] H. Lin and G. M. Rebeiz, "A 70–80-GHz SiGe Amplifier With Peak Output Power of 27.3 dBm," *IEEE Trans. Microw. Theory Techn.*, vol. 64, no. 7, pp. 2039–2049, July 2016.
- [137] Y. Hsiao, Z. Tsai, H. Liao, J. Kao, and H. Wang, "Millimeter-Wave CMOS Power Amplifiers With High Output Power and Wideband Performances," *IEEE Trans. Microw. Theory Techn.*, vol. 61, no. 12, pp. 4520–4533, Dec 2013.
- [138] U. R. Pfeiffer and D. Goren, "A 23-dBm 60-GHz Distributed Active Transformer in a Silicon Process Technology," *IEEE Trans. Microw. Theory Techn.*, vol. 55, no. 5, pp. 857–865, May 2007.
- [139] A. Larie, E. Kerhervé, B. Martineau, L. Vogt, and D. Belot, "A 60 GHz 28 nm UTBB FD-SOI CMOS reconfigurable power amplifier with 21% PAE, 18.2 dBm  $P_{1dB}$  and 74 mW PDC," in *2015 IEEE International Solid-State Circuits Conference - (ISSCC) Digest of Technical Papers*, Feb 2015, pp. 1–3.
- [140] K. Datta and H. Hashemi, "Performance Limits, Design and Implementation of mm-Wave SiGe HBT Class-E and Stacked Class-E Power Amplifiers," *IEEE Journal of Solid-State Circuits*, vol. 49, no. 10, pp. 2150–2171, Oct 2014.
- [141] T. Chi, F. Wang, S. Li, M. Huang, J. S. Park, and H. Wang, "A 60 GHz on-chip linear radiator with single-element 27.9 dBm  $P_{sat}$  and 33.1 dBm peak EIRP using multifeed antenna for direct on-antenna power combining," in *2017 IEEE International Solid-State Circuits Conference (ISSCC)*, Feb 2017, pp. 296–297.
- [142] J. Zhao, M. Bassi, A. Bevilacqua, A. Ghilioni, A. Mazzanti, and F. Svelto, "A 40–67 GHz power amplifier with 13 dBm  $PSAT$  and 16% PAE in 28 nm CMOS LP," in *ESSCIRC 2014 - 40th European Solid State Circuits Conference (ESSCIRC)*, Sep. 2014, pp. 179–182.
- [143] C. R. Chappidi and K. Sengupta, "Frequency Reconfigurable mm-Wave Power Amplifier With Active Impedance Synthesis in an Asymmetrical Non-Isolated Combiner: Analysis and Design," *IEEE Journal of Solid-State Circuits*, vol. 52, no. 8, pp. 1990–2008, Aug 2017.
- [144] B. Koo, Y. Na, and S. Hong, "Integrated Bias Circuits of RF CMOS Cascode Power Amplifier for Linearity Enhancement," *IEEE Trans. Microw. Theory Techn.*, vol. 60, no. 2, pp. 340–351, Feb 2012.
- [145] J. Kim, C. Lee, J. Yoo, and C. Park, "Antiphase method of the cmos power amplifier using pmos driver stage to enhance linearity," *Electronics*, vol. 9, no. 1, p. 103, Jan 2020. [Online]. Available: <http://dx.doi.org/10.3390/electronics9010103>
- [146] H. T. Nguyen and H. Wang, "A Coupler-Based Differential Doherty Power Amplifier with Built-In Baluns for High Mm-Wave Linear-

- Yet-Efficient Gbit/s Amplifications,” in *2019 IEEE Radio Frequency Integrated Circuits Symposium (RFIC)*, June 2019, pp. 195–198.
- [147] H. T. Nguyen, T. Chi, S. Li, and H. Wang, “A Linear High-Efficiency Millimeter-Wave CMOS Doherty Radiator Leveraging Multi-Feed On-Antenna Active Load Modulation,” *IEEE Journal of Solid-State Circuits*, vol. 53, no. 12, pp. 3587–3598, Dec 2018.
- [148] B. Abiri and A. Hajimiri, “A 69-to-79 GHz CMOS multiport PA/radiator with +35.7 dBm CW EIRP and integrated PLL,” in *2018 IEEE International Solid - State Circuits Conference - (ISSCC)*, Feb 2018, pp. 404–406.
- [149] H. T. Nguyen, S. Li, and H. Wang, “A mm-Wave 3-Way Linear Doherty Radiator with Multi Antenna Coupling and On-Antenna Current-Scaling Series Combiner for Deep Power Back-Off Efficiency Enhancement,” in *2019 IEEE International Solid- State Circuits Conference - (ISSCC)*, Feb 2019, pp. 84–86.
- [150] S. Li, T. Chi, J. Park, H. T. Nguyen, and H. Wang, “A 28-GHz Flip-Chip Packaged Chireix Transmitter With On-Antenna Outphasing Active Load Modulation,” *IEEE Journal of Solid-State Circuits*, vol. 54, no. 5, pp. 1243–1253, May 2019.
- [151] J. Chen, L. Ye, D. Titz, F. Giancesello, R. Pilard, A. Cathelin, F. Ferrero, C. Luxey, and A. M. Niknejad, “A digitally modulated mm-Wave cartesian beamforming transmitter with quadrature spatial combining,” in *2013 IEEE International Solid-State Circuits Conference Digest of Technical Papers*, Feb 2013, pp. 232–233.
- [152] S. De Fina, M. Ruggieri, and A. V. Bosisio, “Exploitation of the W-band for high capacity satellite communications,” *IEEE Trans. Aerosp. Electron. Syst.*, vol. 39, no. 1, pp. 82–93, Jan 2003.
- [153] A. Ghosh, T. A. Thomas, M. C. Cudak, R. Ratasuk, P. Moorut, F. W. Vook, T. S. Rappaport, G. R. MacCartney, S. Sun, and S. Nie, “Millimeter-Wave Enhanced Local Area Systems: A High-Data-Rate Approach for Future Wireless Networks,” *IEEE J. Sel. Areas Commun.*, vol. 32, no. 6, pp. 1152–1163, June 2014.
- [154] B. Kim, A. Tran, and J. Schellenberg, “Full W-band power amplifier/combiner utilizing GaAs technology,” in *2012 IEEE/MTT-S International Microwave Symposium Digest*, June 2012, pp. 1–3.
- [155] N. Camilleri, P. Chye, P. Gregory, and A. Lee, “A W-band monolithic amplifier,” in *IEEE International Digest on Microwave Symposium*, May 1990, pp. 903–906 vol.2.
- [156] F. Thome, A. Leuther, M. Schlechtweg, and O. Ambacher, “Broadband High-Power W-Band Amplifier MMICs Based on Stacked-HEMT Unit Cells,” *IEEE Trans. Microw. Theory Techn.*, vol. 66, no. 3, pp. 1312–1318, March 2018.
- [157] Hong-Yeh Chang, Huei Wang, M. Yu, and Yonghui Shu, “A 77-GHz MMIC power amplifier for automotive radar applications,” *IEEE Microw. Wireless Compon. Lett.*, vol. 13, no. 4, pp. 143–145, April 2003.
- [158] M. Morgan and S. Weinreb, “A W-band monolithic medium power amplifier,” in *IEEE MTT-S International Microwave Symposium Digest*, 2003, vol. 1, June 2003, pp. 133–136 vol.1.
- [159] Huei Wang, L. Samoska, T. Gaier, A. Peralta, Hsin-Hsing Liao, Y. C. Leong, S. Weinreb, Y. C. Chen, M. Nishimoto, and R. Lai, “Power-amplifier modules covering 70-113 GHz using MMICs,” *IEEE Trans. Microw. Theory Techn.*, vol. 49, no. 1, pp. 9–16, Jan 2001.
- [160] A. Bessemoulin, M. C. Rodriguez, S. J. Mahon, A. E. Parker, and M. C. Heimlich, “Soldered hot-via E-band and W-band power amplifier MMICs for millimeter-wave chip scale packaging,” in *2016 IEEE MTT-S International Microwave Symposium (IMS)*, May 2016, pp. 1–4.
- [161] A. Barabi, N. Ross, A. Wolfman, O. Shaham, and E. Socher, “A +27 dBm Psat 27 dB Gain W-Band Power Amplifier in 0.1  $\mu\text{m}$  GaAs,” in *2018 IEEE/MTT-S International Microwave Symposium - IMS*, June 2018, pp. 1345–1347.
- [162] V. Radisic, C. Monier, K. K. Loi, and A. Gutierrez-Aitken, “W-Band InP HBT Power Amplifiers,” *IEEE Microw. Wireless Compon. Lett.*, vol. 27, no. 9, pp. 824–826, Sep. 2017.
- [163] R. Majidi-Ahy, C. Nishimoto, M. Riazati, M. Glenn, S. Silverman, S. Weng, Y. Pao, G. Zdasiuk, S. Bandy, and Z. Tan, “100-GHz high-gain InP MMIC cascode amplifier,” *IEEE J. Solid-State Circuits*, vol. 26, no. 10, pp. 1370–1378, Oct 1991.
- [164] D. L. Ingram, Y. C. Chen, J. Kraus, B. Brunner, B. Allen, H. C. Yen, and K. F. Lau, “A 427 mW, 20% compact W-band InP HEMT MMIC power amplifier,” in *1999 IEEE Radio Frequency Integrated Circuits Symposium (Cat No.99CH37001)*, June 1999, pp. 95–98.
- [165] M. Micovic, A. Kurdoghlian, P. Hashimoto, M. Hu, M. Antcliffe, P. J. Willadsen, W. S. Wong, R. Bowen, I. Milosavljevic, A. Schmitz, M. Wetzel, and D. H. Chow, “GaN HFET for W-band Power Applications,” in *2006 International Electron Devices Meeting*, Dec 2006, pp. 1–3.
- [166] Y. Niida, Y. Kamada, T. Ohki, S. Ozaki, K. Makiyama, Y. Minoura, N. Okamoto, M. Sato, K. Joshin, and K. Watanabe, “3.6 W/mm high power density W-band InAlGaIn/GaN HEMT MMIC power amplifier,” in *2016 IEEE Topical Conference on Power Amplifiers for Wireless and Radio Applications (PAWR)*, Jan 2016, pp. 24–26.
- [167] J. M. Schellenberg, “A 2-W W-Band GaN Traveling-Wave Amplifier With 25-GHz Bandwidth,” *IEEE Trans. Microw. Theory Techn.*, vol. 63, no. 9, pp. 2833–2840, Sep. 2015.
- [168] M. Cwiklinski, C. Friesicke, P. Brückner, D. Schwantuschke, S. Wagner, R. Lozar, H. Maßler, R. Quay, and O. Ambacher, “Full W-Band GaN Power Amplifier MMICs Using a Novel Type of Broadband Radial Stub,” *IEEE Trans. Microw. Theory Techn.*, vol. 66, no. 12, pp. 5664–5675, Dec 2018.
- [169] J. Schellenberg, A. Tran, Lani Bui, A. Cuevas, and E. Watkins, “37 W, 75–100 GHz GaN power amplifier,” in *2016 IEEE MTT-S International Microwave Symposium (IMS)*, May 2016, pp. 1–4.
- [170] W. Tai and D. S. Ricketts, “A W-band 21.1 dBm power amplifier with an 8-way zero-degree combiner in 45 nm SOI CMOS,” in *2014 IEEE MTT-S International Microwave Symposium (IMS2014)*, June 2014, pp. 1–3.
- [171] K. Wu, K. Lai, R. Hu, C. F. Jou, D. Niu, and Y. Shiao, “77–110 GHz 65-nm CMOS Power Amplifier Design,” *IEEE Transactions on Terahertz Science and Technology*, vol. 4, no. 3, pp. 391–399, May 2014.
- [172] K. Wang, T. Chang, and C. Wang, “A 1V 19.3dBm 79GHz power amplifier in 65nm CMOS,” in *2012 IEEE International Solid-State Circuits Conference*, Feb 2012, pp. 260–262.
- [173] A. Agah, J. A. Jayamon, P. M. Asbeck, L. E. Larson, and J. F. Buckwalter, “Multi-Drive Stacked-FET Power Amplifiers at 90 GHz in 45 nm SOI CMOS,” *IEEE J. Solid-State Circuits*, vol. 49, no. 5, pp. 1148–1157, May 2014.
- [174] D. Zhao and P. Reynaert, “A 0.9V 20.9dBm 22.3%-PAE E-band power amplifier with broadband parallel-series power combiner in 40nm CMOS,” in *2014 IEEE International Solid-State Circuits Conference Digest of Technical Papers (ISSCC)*, Feb 2014, pp. 248–249.
- [175] T. A. Tran, S. Vehring, Y. Ding, A. Hamidian, and G. Boeck, “Evaluation of transformer and capacitor coupling in W-band broadband CMOS power amplifiers,” in *2016 IEEE MTT-S International Wireless Symposium (IWS)*, March 2016, pp. 1–4.
- [176] J. Jayamon, O. Gurbuz, B. Hanafi, A. Agah, J. Buckwalter, G. Rebeiz, and P. Asbeck, “Spatially power-combined W-band power amplifier using stacked CMOS,” in *2014 IEEE Radio Frequency Integrated Circuits Symposium*, June 2014, pp. 151–154.
- [177] P. Song, M. A. Oakley, A. Ulusoy, M. Kaynak, B. Tillack, G. A. Sadowy, and J. D. Cressler, “A Class-E Tuned W-Band SiGe Power Amplifier With 40.4% Power-Added Efficiency at 93 GHz,” *IEEE Microw. Wireless Compon. Lett.*, vol. 25, no. 10, pp. 663–665, Oct 2015.
- [178] C. M. Armstrong, A. Zubyk, C. Meadows, K. Berg, D. Chan, T. Schoemehl, R. Duggal, N. Hinch, M. Martin, B. Weatherford, B. Tobin, M. Sweeney, and R. Kowalczyk, “A compact G-band MPM power amplifier for high-resolution airborne radar,” in *2017 Eighteenth International Vacuum Electronics Conference (IVEC)*, April 2017, pp. 1–2.
- [179] S. Kim, R. Fan, and F. Dominski, “ViSAR: A 235 GHz radar for airborne applications,” in *2018 IEEE Radar Conference (RadarConf18)*, April 2018, pp. 1549–1554.
- [180] T. S. Rappaport, Y. Xing, O. Kanhere, S. Ju, A. Madanayake, S. Mandal, A. Alkhateeb, and G. C. Trichopoulos, “Wireless Communications and Applications Above 100 GHz: Opportunities and Challenges for 6G and Beyond,” *IEEE Access*, vol. 7, pp. 78 729–78 757, 2019.
- [181] E. Camargo, J. Schellenberg, L. Bui, and N. Estella, “F-Band, GaN Power Amplifiers,” in *2018 IEEE/MTT-S International Microwave Symposium - IMS*, June 2018, pp. 753–756.
- [182] T. B. Reed, Z. Griffith, P. Rowell, M. Field, and M. Rodwell, “A 180mW InP HBT Power Amplifier MMIC at 214 GHz,” in *2013 IEEE Compound Semiconductor Integrated Circuit Symposium (CSICS)*, Oct 2013, pp. 1–4.
- [183] R. Weber, M. Cwiklinski, S. Wagner, R. Lozar, H. Massler, P. Brückner, and R. Quay, “A Beyond 110 GHz GaN Cascode Low-Noise Amplifier with 20.3 dBm Output Power,” in *2018 IEEE/MTT-S International Microwave Symposium - IMS*, June 2018, pp. 1499–1502.
- [184] L. A. Samoska, “An Overview of Solid-State Integrated Circuit Amplifiers in the Submillimeter-Wave and THz Regime,” *IEEE Transactions on Terahertz Science and Technology*, vol. 1, no. 1, pp. 9–24, Sep. 2011.

- [185] V. Radisic, K. M. K. H. Leong, X. Mei, S. Sarkozy, W. Yoshida, P. Liu, J. Uyeda, R. Lai, and W. R. Deal, "A 50 mW 220 GHz power amplifier module," in *2010 IEEE MTT-S International Microwave Symposium*, May 2010, pp. 45–48.
- [186] Z. Griffith, M. Urteaga, and P. Rowell, "A Compact 140-GHz, 150-mW High-Gain Power Amplifier MMIC in 250-nm InP HBT," *IEEE Microw. Wireless Compon. Lett.*, vol. 29, no. 4, pp. 282–284, April 2019.
- [187] S. Diebold, S. Wagner, H. Massler, P. Pahl, A. Leuther, A. Tessmann, T. Zwick, and I. Kallfass, "A Novel  $1 \times 4$  Coupler for Compact and High-Gain Power Amplifier MMICs Around 250 GHz," *IEEE Trans. Microw. Theory Techn.*, vol. 63, no. 3, pp. 999–1006, March 2015.
- [188] A. B. Amado-Rey, Y. Campos-Roca, F. van Raay, C. Friesicke, S. Wagner, H. Massler, A. Leuther, and O. Ambacher, "Analysis and Development of Submillimeter-Wave Stacked-FET Power Amplifier MMICs in 35-nm mHEMT Technology," *IEEE Transactions on Terahertz Science and Technology*, vol. 8, no. 3, pp. 357–364, May 2018.
- [189] M. Furqan, F. Ahmed, B. Heinemann, and A. Stelzer, "A 15.5-dBm 160-GHz High-Gain Power Amplifier in SiGe BiCMOS Technology," *IEEE Microw. Wireless Compon. Lett.*, vol. 27, no. 2, pp. 177–179, Feb 2017.
- [190] Zuo-Min Tsai, Hsin-Chiang Liao, Yuan-Hong Hsiao, Huei Wang, J. Y. Liu, M. F. Chang, Yu-Ming Teng, and Guo-Wei Huang, "A 1.2V broadband D-band power amplifier with 13.2-dBm output power in standard RF 65-nm CMOS," in *2012 IEEE/MTT-S International Microwave Symposium Digest*, June 2012, pp. 1–3.
- [191] D. Simic and P. Reynaert, "A 14.8 dBm 20.3 dB Power Amplifier for D-band Applications in 40 nm CMOS," in *2018 IEEE Radio Frequency Integrated Circuits Symposium (RFIC)*, June 2018, pp. 232–235.
- [192] H. S. Son, C. J. Lee, D. M. Kang, T. H. Jang, H. S. Lee, S. H. Kim, C. W. Byeon, and C. S. Park, "A D-band CMOS power amplifier for wireless chip-to-chip communications with 22.3 dB gain and 12.2 dBm P1dB in 65-nm CMOS technology," in *2018 IEEE Topical Conference on RF/Microwave Power Amplifiers for Radio and Wireless Applications (PAWR)*, Jan 2018, pp. 35–38.
- [193] K. W. Brown, D. M. Gritters, and H. Kazemi, "W- and G-Band Solid State Power Combining," in *2015 IEEE Compound Semiconductor Integrated Circuit Symposium (CSICS)*, Oct 2015, pp. 1–4.
- [194] X. Mei, W. Yoshida, M. Lange, J. Lee, J. Zhou, P. Liu, K. Leong, A. Zamora, J. Padilla, S. Sarkozy, R. Lai, and W. R. Deal, "First Demonstration of Amplification at 1 THz Using 25-nm InP High Electron Mobility Transistor Process," *IEEE Electron Device Lett.*, vol. 36, no. 4, pp. 327–329, April 2015.
- [195] J. Langst, S. Diebold, H. Massler, S. Wagner, A. Tessmann, A. Leuther, T. Zwick, and I. Kallfass, "Balanced medium power amplifier MMICs from 200 to 270 GHz," in *2013 38th International Conference on Infrared, Millimeter, and Terahertz Waves (IRMMW-THz)*, Sep. 2013, pp. 1–3.
- [196] I. Kallfass, P. Pahl, H. Massler, A. Leuther, A. Tessmann, S. Koch, and T. Zwick, "A 200 GHz Monolithic Integrated Power Amplifier in Metamorphic HEMT Technology," *IEEE Microw. Wireless Compon. Lett.*, vol. 19, no. 6, pp. 410–412, June 2009.
- [197] B. Schoch, A. Tessmann, A. Leuther, S. Wagner, and I. Kallfass, "260 GHz Broadband Power Amplifier MMIC," in *2019 12th German Microwave Conference (GeMiC)*, March 2019, pp. 232–235.
- [198] N. Sarmah, P. Chevalier, and U. R. Pfeiffer, "160-GHz Power Amplifier Design in Advanced SiGe HBT Technologies With  $P_{\text{sat}}$  in Excess of 10 dBm," *IEEE Trans. Microw. Theory Techn.*, vol. 61, no. 2, pp. 939–947, Feb 2013.
- [199] J. Al-Eryani, H. Knapp, J. Wursthorn, K. Aufinger, S. Majied, Hao Li, S. Boguth, R. Lachner, J. Böck, and L. Maurer, "A 162 GHz power amplifier with 14 dBm output power," in *2016 IEEE Bipolar/BiCMOS Circuits and Technology Meeting (BCTM)*, Sep. 2016, pp. 174–177.
- [200] M. Bao, Z. S. He, and H. Zirath, "A 100–145 GHz area-efficient power amplifier in a 130 nm SiGe technology," in *2017 47th European Microwave Conference (EuMC)*, Oct 2017, pp. 1017–1020.
- [201] S. Daneshgar and J. F. Buckwalter, "Compact Series Power Combining Using Subquarter-Wavelength Baluns in Silicon Germanium at 120 GHz," *IEEE Trans. Microw. Theory Techn.*, vol. 66, no. 11, pp. 4844–4859, Nov 2018.
- [202] D. Parveg, M. Varonen, D. Karaca, A. Vahdati, M. Kantanen, and K. A. I. Halonen, "Design of a D-Band CMOS Amplifier Utilizing Coupled Slow-Wave Coplanar Waveguides," *IEEE Trans. Microw. Theory Techn.*, vol. 66, no. 3, pp. 1359–1373, March 2018.



**Vittorio Camarchia** (S'01–M'04–SM'14) was born in Turin, Italy, in 1972. He received the Laurea degree and Ph.D. degree in Electronic Engineering from the Politecnico di Torino, Turin, Italy, in 2000 and 2003, respectively. He was a Visiting Researcher with the Electrical and Computer Engineering Department, Boston University. Since 2004 he joined the Department of Electronics and Telecommunications of the Politecnico di Torino where is presently an Associate Professor. His research is focused on modeling, design and characterization of RF and microwave modules and systems. His research has been supported by the European Space Agency (ESA), and is presently an external reviewer for space related calls for the Research Executive Agency of the European Commission. He has published 160 peer-reviewed papers, two books and several book chapters. He is member of the IEEE MTT-S Subcommittees #12 on power amplifiers and #23 on Wireless Communications and serves as member of the International Microwave Symposium Technical Program Review Committee on power amplifiers. He has organized several WS and Focused Sessions at EuMW and IMS on nonlinear measurements, microwave backhaul, 5G and millimeter (mm)-wave applications, and mm-wave power amplifier design. He also served as a guest editor of the IEEE Transactions on Microwave Theory and Techniques Special Issues on Broadband Millimeter-wave Power Amplifiers (2020). Prof. Camarchia was a recipient of the 2002 Young Graduated Research Fellowship presented by the GAAS Association.



**Roberto Quaglia** (M'13) was born in Casale Monferrato, Italy, in 1984. He received the Laurea degree (cum laude) in electronic engineering and Ph.D. degree in electronic devices from the Politecnico di Torino, Turin, Italy, in 2008 and 2012, respectively. He is currently a Lecturer with the School of Engineering of Cardiff University, Wales, U.K. His current research interests include the design, modelling, and predistortion of high-efficiency MMIC power amplifiers. Dr. Quaglia was a recipient of the European Union Marie Skłodowska Curie Fellow in 2015 and the 2009 Young Graduated Research Fellowship presented by the GAAS Association.



**Anna Piacibello** (S'15–M'20) was born in Chivasso, Italy, in 1991. She received the Bachelor and Master degrees in Electronic Engineering from the Politecnico di Torino in 2013 and 2015, respectively. In 2017, she was a visiting researcher at the Centre for High Frequency Engineering (CHFE) of Cardiff University. She received the PhD degree cum laude in Electric, Electronic and Communication Engineering from the Politecnico di Torino in 2019. Her current research interests include broadband and highly efficient microwave power amplifiers. Dr.

Piacibello is currently a postdoctoral research associate with the Department of Electronics, University of Rome Tor Vergata, Italy. She was a recipient of the 2018 Young Engineer Prize awarded by the EuMA association.





**Duy P. Nguyen** (M'17) received the B.S. degree (with highest honors) in electrical and electronics engineering from Vietnam National University, Ho Chi Minh City, Vietnam, in 2011, and the M.S. and Ph.D. degrees in electrical and computer engineering from the University of California, Davis, CA, USA, in 2014 and 2017, respectively. In 2017, he joined MACOM Technology Solutions Inc., Santa Clara, CA, USA, as a Senior Design Engineer where he designs optical linear drivers, and other RFICs and analog circuits. He has developed and designed a number of RFICs and MMICs in GaAs, GaN, InP, SiGe, and CMOS including power amplifiers, wideband distributed amplifiers, Doherty amplifiers, LNAs, T/R switches, phase shifters, fully integrated front-end modules, and linear drivers for optical modulators. He has authored and co-authored more than 30 patents, journals and conference papers. Dr. Nguyen was a recipient of Anil Jain Award for the best Ph.D. dissertation from UC Davis, Spot Recognition Award from MACOM in 2018, and Vietnam Education Foundation (VEF) fellowship.



**Anh-Vu Pham** (SM'03) received the B.E.E. (with highest honors), M.S., and Ph.D. degrees in electrical engineering from the Georgia Institute of Technology, Atlanta, in 1995, 1997, and 1999, respectively. Anh-Vu joined the University of California at Davis in 2002 as an Assistant Professor and was promoted to full Professor in 2008. From 1999 to 2002, he was an Assistant Professor at Clemson University. Anh-Vu is conducting research in RF to THz hybrid and integrated circuits, especially power amplifiers, antennas, radar and sensors, and energy harvesting systems. His research has been supported by DARPA, National Science Foundation, Office of Naval Research, Air Force Research Laboratory, Lawrence Livermore National Laboratory, and numerous companies. He has published 200 peer-reviewed papers, several book chapters, and two books and has graduated 21 Ph.D. students. Anh-Vu served as the Co-chair of Technical Program Committee of the IEEE International Microwave Symposium, 2016 in San Francisco, Co-Chair of the Technical Program Committee for the IEEE Asia Pacific Microwave Conference, 2017 in Malaysia, an IEEE MTT-S Distinguished Microwave Lecturer (2010-2012), and member/chair of International Microwave Symposium Technical Program Review Committee on power amplifiers. He also served as a guest editor of the IEEE Transactions on Microwave Theory and Techniques Special Issues on Broadband Millimeter-wave Power Amplifiers (2020) and Asia-Pacific Microwave Conference (2017). He received the National Science Foundation CAREER Award in 2001 and Outstanding Young Engineer Award from the IEEE Microwave Theory and Techniques Society, 2008. Anh-Vu is currently a co-director of the Davis Millimeter Wave Research Center. In 1997, Anh-Vu co-founded RF Solutions, a fabless semiconductor company providing power amplifiers and RFICs for WiFi applications. In 2003, RF Solutions was acquired by Anadigics. In 2008, he co-founded Planarmag, Inc and served as the CTO. In 2010, Planarmag, Inc was successfully acquired by TE Connectivity.



**Hua Wang** (M'05–SM'15) is an associate professor at the School of Electrical and Computer Engineering (ECE) at Georgia Institute of Technology and the director of Georgia Tech Electronics and Micro-System (GEMS) lab. Prior to that, he worked at Intel Corporation and Skyworks Solutions on mm-Wave integrated circuits and RF front-end modules. He received his M.S. and Ph.D. degrees in electrical engineering from the California Institute of Technology, Pasadena, in 2007 and 2009, respectively. Dr. Wang is interested in innovating analog, mixed-signal, RF, and mm-Wave integrated circuits and hybrid systems for wireless communication, sensing, and bioelectronics applications. He has authored or co-authored over 160 peer-reviewed journal and conference papers. Dr. Wang received the DARPA Young Faculty Award in 2018, the National Science Foundation CAREER Award in 2015, the IEEE MTT-S Outstanding Young Engineer Award in 2017, the Georgia Tech Sigma Xi Young Faculty Award in 2016, the Georgia Tech ECE Outstanding Junior Faculty Member Award in 2015, and the Lockheed Dean's Excellence in Teaching Award in 2015. He held the Demetrius T. Paris Professorship from 2014 to 2018. His GEMS research group has won multiple academic awards and best paper awards, including the 2019 Marconi Society Paul Baran Young Scholar, the IEEE RFIC Best Student Paper Awards (1st Place in 2014, 2nd Place in 2016, and 2nd Place in 2018), the IEEE CICC Outstanding Student Paper Awards (2015, 2018, and 2019), the IEEE CICC Best Conference Paper Award (2017), the 2016 IEEE Microwave Magazine Best Paper Award, and the IEEE SENSORS Best Live Demo Award (2nd Place in 2016). Dr. Wang is a Technical Program Committee (TPC) Member for IEEE ISSCC, RFIC, CICC, and BCICTS conferences. He is a Steering Committee Member for IEEE RFIC and CICC. He is the Conference Chair for CICC 2019 and Conference General Chair for CICC 2020. He is a Distinguished Lecturer (DL) for the IEEE Solid-State Circuits Society (SSCS) for the term of 2018-2019. He serves as the Chair of the Atlanta's IEEE CAS/SSCS joint chapter that won the IEEE SSCS Outstanding Chapter Award in 2014.